TRIBHUVAN UNIVERSITY

INSTITUTE OF ENGINEERING

PULCHOWK CAMPUS

B-06-BME-2019-2024

AERODYNAMIC ANALYSIS AND PERFORMANCE STUDY OF MODIFIED HYBRID WIND TURBINE WITH HELICAL SAVONIUS AND H-TYPE DARRIEUS ROTOR

Submitted by:

BIRAT DUWADI

SAMIR SHRESTHA

SUJAN DHAKAL

SURAJ WAGLE

A PROJECT REPORT SUBMITTED TO THE DEPARTMENT OF MECHANICAL AND AEROSPACE ENGINEERING IN PARTIAL FULFILLMENT OF THE REQUIREMENT

DEPARTMENT OF MECHANICAL AND AEROSPACE ENGINEERING

LALITPUR, NEPAL

APRIL, 2024

COPYRIGHT

TRIBHUVAN UNIVERSITY

INSTITUTE OF ENGINEERING

PULCHOWK CAMPUS

DEPARTMENT OF MECHANICAL AND AEROSPACE ENGINEERING

The undersigned certify that they have read, and recommended totheInstitute of Engineering for acceptance, a project report entitled "AERODYNAMIC ANALYSIS AND PERFORMANCE STUDY OF MODIFIED HYBRID WIND TURBINE WITH HELICAL SAVONIUS AND H-TYPE DARRIEUS ROTOR" submitted byBirat Duwadi, Samir Shrestha, Sujan Dhakal and Suraj Wagle in partial fulfillment of the requirements for the degree of Bachelor of Mechanical Engineering.

Supervisor, Laxman Motra

Assistant Professor

Department of Mechanical and Aerospace Engineering

IOE, Pulchowk Campus

01/17

External Examiner, Er. Salim Maharjan

Lecturer

Himalaya College of Engineering

Tribhuvan University
Institute of Engineering
Department of Mechanical and Aerospace Engg.
Pulchowk Campus

Committee Chairperson, Dr. Sudip Bhattrai

Head

Department of Mechanical and Aerospace Engineering

IOE, Pulchowk Campus

Date: 2024/04/29

ABSTRACT

This report aims to explore the potential of combining the Darrieus and Savonius vertical axis wind turbine (VAWT) designs to create a more efficient and versatile renewable energy solution. The Darrieus VAWT is known for its high efficiency in capturing wind energy, while the Savonius VAWT exhibits excellent self-starting capabilities and performs well in low wind conditions. By combining these two designs, we aim to leverage their respective advantages and overcome their individual limitations. The present report introduces a CFD analysis of a proposed hybrid VAWT using ANSYS Fluent and experimental analysis. Straight blade with airfoil profile S1046 was used for darrieus rotor. The hybrid rotor has a helical Savonius rotor with 3 Darrieus blades. The performance study of hybrid rotor at different radius ratios are carried out and highest power coefficient is achieved at 0.43 radius ratio. It is found that radius ratio greatly affects the performance of the turbine. The larger the diameter of Savonius rotor, more is the interaction of Savonius and Darrieus blades resulting loss in performance. The final optimized design is fabricated and experimentally tested. From the data obtained experimentally, Hybrid rotor so fabricated has been found to operate at low wind speed of 4.425 m/s which signifies its low self-starting speed. The maximum rpm of the rotor blade is recorded to be 852.166 rpm at the wind speed of 10.863 m/s signifying its ability to perform at high wind speed. The performance of solo Darrieus (Cp=0.291) and solo Savonius rotor (Cp =0.219) are then compared with the hybrid one (Cp=0.286) and found that the hybrid rotor has the ability to attain the peak performance close to Darrieus rotor.

Keywords: Hybrid VAWT, CFD, Helical Savonius rotor, Radius ratio, Power coefficient

TRIBHUVAN UNIVERSITY

INSTITUTE OF ENGINEERING

PULCHOWK CAMPUS

DEPARTMENT OF MECHANICAL AND AEROSPACE ENGINEERING

The undersigned certify that they have read, and recommended totheInstitute of Engineering for acceptance, a project report entitled "AERODYNAMIC ANALYSIS AND PERFORMANCE STUDY OF MODIFIED HYBRID WIND TURBINE WITH HELICAL SAVONIUS AND H-TYPE DARRIEUS ROTOR" submitted byBirat Duwadi, Samir Shrestha, Sujan Dhakal and Suraj Wagle in partial fulfillment of the requirements for the degree of Bachelor of Mechanical Engineering.

Supervisor, Laxman Motra

Assistant Professor

Department of Mechanical and Aerospace Engineering

IOE, Pulchowk Campus

01/17

External Examiner, Er. Salim Maharjan

Lecturer

Himalaya College of Engineering

Tribhuvan University
Institute of Engineering
Department of Mechanical and Aerospace Engg.
Pulchowk Campus

Committee Chairperson, Dr. Sudip Bhattrai

Head

Department of Mechanical and Aerospace Engineering

IOE, Pulchowk Campus

Date: 2024/04/29

ACKNOWLEDGEMENT

First of all, we would like to express our deepest gratitude to the Department of Mechanical and Aerospace Engineering, IOE, Pulchowk Campus, for providing us with the opportunity to work on a project to enhance our knowledge and skill and also gain a valuable experience in the related field.

Similarly, we would like to thank our supervisor, Assistant Professor Laxman Motra for his guidance and motivation. We are indebted to him for providing his valuable insights and always encouraging and motivating us. It certainly wouldn't have been possible without him.

Finally, we would also like to extend thanks to all our friends and seniors especially Mr. Anup Pandey who helped us with our CFD analysis.

TABLE OF CONTENTS

LIST OF FIGURES

LIST OF TABLES

LIST OF ACRONYMS AND ABBREVIATIONS

AR	Aspect Ratio
CAD	Computer Aided Design
Cp	Power coefficient
Ct	Torque coefficient
HAWT	Horizontal axis wind turbine
OR	Overlap ratio
CFD	Computational Fluid Dynamics
TSR	Tip Speed Ratio
VAWT	Vertical Axis Wind Turbine
RANS-SA	Reynolds-Averaged Navier-Stokes with Spalart-Allmaras turbulence model

SYMBOLS

A	Area of wind turbine rotor (in sq.meter)
D	diameter of Darrieus rotor (in meter)
Ds	diameter of Savonius rotor (in meter)
Do	diameter of end plate (in meter)
H	height of Darrieus rotor (in meter)
Hs	height of Savonius rotor (in meter)
N	Number of blades
C	length of blade chord
Cp	coefficient of power
ρ	Air density (kg/m3)
	Attachment angle (◦)

CHAPTER 1: INTRODUCTION

Wind turbine is an efficient solution for green energy production as they utilize a renewable and abundant resource, generate electricity without emissions or pollution, and contribute to a sustainable and clean energy future. However, traditional wind turbines have limitations in capturing wind energy efficiently due to their design constraints and dependency on specific wind directions. To overcome these limitations, the proposed project aims to combine the advantages of the Helical Savonius and Darrieus turbine designs to create a hybrid system that maximizes energy extraction from wind resources.

1.1 Background:

1.1.1 Vertical axis wind turbine

A Vertical Axis Wind Turbine (VAWT) is a type of a wind turbine that has its rotor blade shaft oriented in a vertical direction. This type of turbine accepts the wind from any direction without any use of yoke mechanism. The vertical arrangement of rotor shaft allows the generator and gearbox to be located close to the ground which facilitates for easy service and maintenance. The simpler design of VAWTs allows it to be used in any household applications to produce required amount of electricity. The operation of this type of turbine is quieter due to the slower blade tip speed that allows it to be dynamic in application, be it residential or industrial zone.

Horizontal Axis Wind Turbines and Vertical Axis Wind Turbine differ in their design, efficiency, and suitability for different applications. One significant advantage of VAWTs over HAWTs is their ability to capture wind from any direction which makes them suitable for urban or confined areas where wind direction is unpredictable. Wind patterns in urban environments are much more chaotic and fuller of turbulence. The VAWTs have a relatively low environmental impact and better adaptable characteristics to the unsteady wind of urban terrains and are relatively simple in design to integrate with urban buildings and infrastructure. Additionally, VAWTs have a compact design making them easier to install and maintain. They are also less vulnerable to storms and can operate in turbulent wind conditions. Generally, HAWTs have higher efficiency

compared to VAWTs. Their horizontal design allows them to capture wind more effectively, resulting in better energy conversion. They are commonly used in large-scale wind farms. VAWTs have lower efficiency compared to HAWTs. Their vertical design and variable wind speeds along the blades lead to lower energy conversion. They are often used for small-scale or distributed applications. HAWTs have a larger visual impact compared to VAWTs due to their size and spinning blades. They are often visible from a distance, which can be a consideration in certain landscapes or residential areas. VAWTs have a smaller visual footprint and are less obtrusive. Their vertical design and compact size make them visually more appealing, especially in urban and residential settings.

Based on their mode of operation, the different types of vertical axis wind turbines are: -

- Drag-type vertical axis wind turbine.
- Lift-type vertical axis wind turbine.

1.1.2 Drag-type vertical axis wind turbine

A drag type Vertical Axis Wind Turbine is a specific design of VAWT that works on the principle of drag force created by the incoming air. In this type of turbine, the rotor blades are designed to create resistance to the wind causing the blade to rotate which in turn converts wind energy into mechanical energy. Drag-type VAWTs have a simpler design, making them potentially easier to manufacture and maintain. They can also operate efficiently at lower wind speeds, making them suitable for regions with lower average wind speed.

Savonius Wind Turbine is a drag-type Vertical Axis Wind Turbine. The shape is made up of two semi-cylinders that are rotated 90 degrees with respect to each other and positioned on the outside of the axis. The wind turbine is simple to get going because of the difference in drag between the convex (low drag) and concave (high drag) sides. The efficiency of a Savonius Vertical Axis Wind Turbine (VAWT) can vary depending on the specific design characteristics, wind conditions, and operational parameters. The helical Savonius VAWT has curved blades in a form of helical or twisted shape around the rotor axis. The helical design offers many advantages, including improved self-

starting capabilities, increased torque generation, enhanced efficiency compared to traditional straight-bladed Savonius designs. The traditional Savonius VAWTs with cup-like blades often exhibit lower efficiency compared to helical design due to their higher drag and lower torque generation. They generally have lower self-starting capabilities and are less effective in capturing wind energy at lower wind speeds.

Figure 1.1 Traditional Savonius VAWT

Source: https://www.archiexpo.com/prod/windside/product-88530-959470.html?fbclid=IwAR3lA_YKbLnXG6HhD1bMg-A5TGP3SmwLvXdKgh1iT3_t2f_9CPl4WmAvtwk, accessed 30 june 2023

Figure 1.2 Helical Savonius VAWT

Source: https://www.pinterest.com/pin/8725793021520319/, Accessed 30 june 2023

1.1.3 Lift-type Vertical Axis Wind Turbine

A Lift-type Vertical Axis Wind Turbine is a type of VAWT that works on the principle of Coanda effect and the pressure difference. In Lift-type VAWT, the rotor blades are designed to generate lift, similar to the wings of an aircraft, as the wind flows over them which creates lift force to causes the turbine to rotate and convert wind energy into rotational mechanical energy.

Darrieus wind turbine is an example of Lift-type Vertical Axis Wind Turbine. On the basis of blade design, it is classified into three types: -

a) Classic Darriues Wind Turbine

   This is the traditional design of a Darrieus turbine, consisting of a vertical axis with two or more airfoil-shaped blades that are curved in semi-circular or “D”

shape. The blades are connected to the central shaft and generate lift as the wind flows over them.

b) H-rotor Darrieus Wind Turbine

The H-rotor design consists of two or more airfoil shaped blades arranged in "H" shape. The blades are connected to the central shaft and generate lift by capturing the wind coming from any direction.

c) Helical Darrieus Wind Turbine

The Helical Darrieus Wind Turbine is a type of vertical axis wind turbine with twisted or helical blades. It has improved starting performance, increased aerodynamic efficiency, operates quietly, and capture wind from multiple directions.

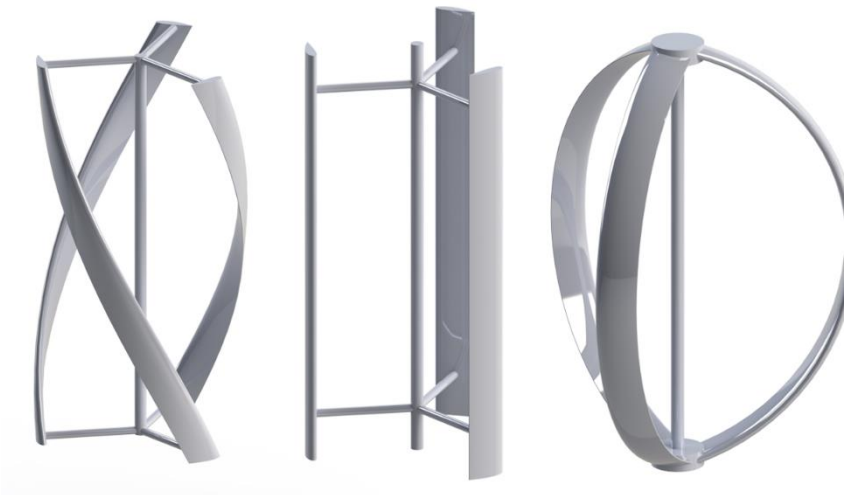

Figure 1.3 Types of Darrieus VAWT

Source: https://www.pinterest.com/pin/191754896613600746/?fbclid=IwAR3rmSdk1xs6mkT618DXa, mpotfkPCmdhl9D3KyOiSRbkl5rzSRM6JWLRWZs, accessed 30 june 2023

1.1.4 Hybrid Vertical Axis Wind Turbine

A hybrid VAWT (Vertical Axis Wind Turbine) refers to a wind turbine design that combines the characteristics and features of both the Savonius and Darrieus turbine designs into a single system. The deficiencies and limitations of individual wind turbine designs have led researchers to explore combined designs that overcome these challenges. For the Darrieus VAWT, efforts have been made to improve its self-starting capability by incorporating twisted and chambered blades and modifying the blade trajectory. However, these modifications often result in complex shapes that are difficult to manufacture, lower energy harvesting efficiency, and the need for complex control systems, leading to increased operation and maintenance costs.

Similarly, for the Savonius VAWT, attempts have been made to increase its efficiency through blade shape optimization, twisting, and the use of shielding obstacles or curtains to modify the pressure distribution over the blade. However, these modifications suffer from similar drawbacks as those for the Darrieus VAWT, and the improved efficiency is usually much less compared to the Darrieus design.

To address these deficiencies, researchers have developed hybrid Savonius-Darrieus wind turbine designs. The hybrid turbine integrates both designs to leverage their respective advantages. The Savonius section of the hybrid turbine provides self-starting capability, ensuring operation even at low wind speeds where the Darrieus section may face challenges initiating motion. Additionally, the drag-based operation of the Savonius section adds robustness and simplicity to the overall design.

By integrating these two designs, the hybrid turbine aims to optimize power generation and expand its suitability across different wind conditions. This innovative approach represents a significant advancement in VAWT design, seeking to enhance the efficiency and performance of wind turbines for renewable energy generation. Therefore, a hybrid Savonius-Darrieus type vertical axis wind rotor offers several advantages over individual Savonius or Darrieus wind rotors. It combines the high starting torque of the Savonius rotor with the high-power coefficient of the Darrieus rotor, creating a synergistic combination of these designs. This hybrid configuration has

the potential to address the limitations of individual designs and maximize the efficiency and effectiveness of wind energy generation.

Various configurations of combined turbines have been explored by researchers, aiming to optimize the interaction between the Savonius and Darrieus sections. These configurations are continually evolving, with ongoing research focusing on finding the most efficient and effective arrangements to harness wind power effectively.

Figure 1.4 Hybrid VAWT

Source:https://www.globalsources.com/product/wind-turbine-power-system_1051227360f.htm?fbclid=IwAR16_jZjhVt_1yK9GLaD6Pl8Nt-VUa97bbcUONT6FAxIgJEOqR1Ru00XLH4, accessed 30 june 2023

1.2 Problem statement

In recent years, the utilization of renewable energy sources, particularly wind power has gained significant attention in the field of sustainable energy systems. Wind turbines mainly Vertical Axis Wind Turbines (VAWTs) have received more attention due to its suitability for residential and urban applications, omnidirectional wind capture, and ease of maintenance. However, traditional VAWTs face challenges related to their efficiency and power generation capacity. The Helical-type Savonius and H-type Darrieus VAWT configurations are two prominent designs that have been studied extensively over the years. The Savonius design, characterized by its helical rotor, exhibits good starting characteristics compared to cup-like blades and operates

effectively at low wind speeds. On the other hand, the Darrieus design with its curved or airfoil-shaped blades provides higher efficiency at higher wind speeds but requires higher wind speeds to start rotating. While both designs have their own advantages which provides an opportunity to combine the strengths of both designs to create a more efficient and effective wind turbine system. By integrating these two configurations, it is possible to achieve enhanced power generation, improved efficiency, and increased energy capture across a wider range of wind speeds.

Therefore, the problem to be addressed in this project is to design, optimize, and evaluate a hybrid VAWT that overcomes the limitations of traditional VAWTs and maximize energy generation efficiency, improve starting characteristics, and enhance overall performance.

1.3 Objectives:

1.3.1 Main Objective

- To design, fabricate and experimentally explore the performance of a helical-type Savonius and H-type Darrieus hybrid wind turbine.

1.3.2 Specific Objectives:

- To analyze and optimize the performance of the hybrid VAWT through computational simulations.
- To fabricate a scaled-down prototype of the hybrid VAWT and evaluate its performance through experimental testing under various wind conditions.
- To compare the performance of the hybrid VAWT with individual VAWT designs i.e. Helical-type Savonius and H-type Darrieus VAWT.

1.4 Scope of work:

a) It can be uniquely advantageous to deploy VAWTs in urban environments due to their ability to efficiently capture turbulent and multi-directional winds, making them well-suited for generating wind energy in cities.

b) It can be conveniently installed on rooftops, making it an ideal choice for rooftop installations in densely populated areas, thanks to its compact size and vertical axis design.

c) It can be particularly beneficial in low wind speed areas, as it is capable of generating electricity even in conditions where traditional vertical axis wind turbines may struggle to produce sufficient power.

d) It can be a viable solution for off-grid applications, providing a decentralized and sustainable energy source for remote locations or areas with limited access to the electrical grid.

e) It can be effectively integrated into hybrid renewable energy systems, allowing for the combination of wind power with other energy sources such as solar or storage systems.

CHAPTER 2: LITERATURE REVIEW

2.1 Savonius turbine

The Savonius rotor type presents its disposition in the “S” form along its vertical axis which the rotation occurs mainly due to the drag force provided by the wind in its concave and convex buckets. It has the advantage of not needing an orientation system according to the wind direction, therefore, suitable to operate in urban centers due to its good response even to fast changes in wind direction. Two-stage rotors had higher power coefficients with respect to one and three-stage rotors. A comparison between the helical geometry and the conventional Savonius rotor reveals that the helical design performs better. It is observed that the helical Savonius rotor's performance is sensitive to the Reynolds number. The coefficient of power can be improved from 0.12-0.18 to 0.52 with the improvements in Blade shape, i.e. Helical blade. The helical turbine performing slightly better in terms of maximum power coefficient, 9.4% higher in experimental comparison. The helical turbine demonstrated better performance and stability in torque generation when manufacturing complexity is not a concern [1]. Increasing the overlap distance of the helical Savonius rotor reduces velocity, worsens total pressure distribution, and subsequently decreases net torque. Average torque coefficient and maximum power coefficient decrease as well. The optimal rotor design is non-overlapped blades, yielding a maximum power coefficient (Cp max) of 0.124 at λ=0.73. For Improved performance, a novel helical Savonius rotor design with delta blades is proposed, resulting in improved velocity, pressure distribution, and produced torque. A significant improvement of 14.51% in the maximum power coefficient is achieved [2].

The use of both upper and lower end plates results in a significant increase in power coefficient by 36% compared to no end plates. The study finds that the maximum power coefficient and tip speed ratio of helical Savonius wind turbines increase linearly with the end plate area. Circular end plates are identified as the best choice for maximizing power and torque coefficients for helical Savonius wind turbines. The use of both upper and lower circular end plates leads to a significant 36% increase in the power coefficient compared to no end plate [4]. The surface pressure distribution around the blade showed

that the convex blade facing the flow experienced the maximum surface pressure, while the concave blade had the minimum. During blade rotation, some sections exhibited effective torque, while others experienced a relative drag force, which slowed down the rotation of the blades [5].

2.2 Darrieus wind turbine

The Darrieus wind rotor is a type of vertical axis wind turbine that shows promise for generating wind power in areas with low and gentle wind speeds, particularly in remote or residential locations.

H-Darrieus rotors are gaining popularity in unconventional situations due to its simpler manufacturing and straight blade design, and believed to perform better when the wind flow is not aligned with the rotor's axis. These rotors are expected to work even more efficiently when the wind comes from different directions [6]– [8]. It is feasible to shape blades of Darrieus turbine with a streamlined cross-section similar to the wings of birds. By giving the blades a streamlined shape, they can efficiently convert the maximum available energy from the fluid into mechanical energy by utilizing the forward motion and minimizing resistance. When a turbine is running at lower Tip Speed Ratios (TSRs), particularly below 5, the angle at which the wind hits the turbine blades fluctuates more. This increased variation in the angle of attack creates the potential for dynamic stall to occur. Dynamic stall refers to a phenomenon where the stall angle of the airfoil is delayed, allowing it to generate higher lift coefficients and operate within a broader range before stalling again at a later point. Darrieus wind turbine with a higher solidity, meaning a larger number of blades, or those with three blades generally outperform turbines with only two blades across most operating conditions [9]. The S-1046 airfoil has been found to be the optimal choice for achieving higher efficiency, specifically in terms of power coefficient, compared to the standard NACA 0018 airfoil commonly used in previous designs of Darrieus turbines. This means that using the S-1046 airfoil results in a relative increase in power coefficient of about 26.83%. In the case of an H-rotor Darrieus turbine with the S-1046 airfoil, the torque coefficient and power coefficient were evaluated at various speed ratios, while maintaining a constant solidity of 0.1 [10].

2.3 Hybrid VAWT

Gupta et al. [11] made a combined VAWT and compared the results obtained with the individual rotors. They observed a significant improvement in the power coefficient for the hybrid Savonius and Darrieus rotor. Feng et al. [12] reported that H-rotor is self-started at low tip speed ratio in combined VAWT. investigated the performance of combined VAWT comprised of a three bucket H-rotor wind turbine with DUW200 airfoils was investigated [13]. It concluded that when H-rotor and Savonius were combined, a higher performance was obtained as compared to the H-rotor only. The study of combined VAWT to improve the coefficient of power with same AR showed that the modified hybrid turbine gave higher coefficient of power (0.23) at a low wind speed, as compared to that of Savonius rotor (0.19) and Darrieus three blade rotor (0.21) [14]. Pallotta et al. [15] conducted experiments on a hybrid rotor setup to enhace its efficiency under low and medium wind velocities. This hybrid setup exhibited a favorable performance across various operational conditions as compared to solo Savonius or solo Darrieus rotor. The results from studies of impact of attachment angle and radius ratio showed that there was a significant influence of radius ratio on the hybrid turbine performance. [16] [17]. Similarly, Ali et al. [18] investigated on how the position of Savonius and Darrieus wind turbines affects the performance of a hybrid wind turbine under low wind speeds, using both numerical simulations and experiments. The efficiency of the suggested hybrid wind turbine was obtained 51.2% which was better compared to wind turbine of other specifications. An experiment to assess how different arrangements affect the efficiency of a hybrid wind turbine was carried out. The experiment showed that the configuration with the Savonius rotor positioned in the center of the Darrieus wind turbine had the maximum level of performance compared to other arrangements. This particular configuration achieved a maximum coefficient of power of 0.2 when the wind speed ratio (λ) was 0.86 [19].

The literature mentioned above explores the use of hybrid vertical axis wind turbine to achieve high starting torque. By integrating Darrieus blades with helical Savonius blades, the self-starting ability and the overall efficiency of the turbine improves. Moreover, the performance of the hybrid rotor is greatly influenced by various geometric parameters, which depend on the shape of the airfoil profile. Therefore, the

unique aspect of this study is the introduction of a new idea for a hybrid wind rotor which combines the helical Savonius blades with suitable Darrieus blades.

2.4 Performance parameters

a) Wind power: $P = \frac{1}{2} \rho A V^3$

b) Aspect ratio: α = Rotor Height / Rotor Diameter

c) Non-dimensional chord length: chord length / rotor diameter

d) Radius ratio: $\beta = Rs/R$ where, Rs & R are radius of Savonius & Darrieus rotors respectively

e) Reynolds number:

$$R_e = \frac{\rho V D}{\mu}$$

f) Tip speed ratio:

TSR is the ratio between speed of tip blade and wind speed through the blade; TSR is determined as follows.

$$\lambda = \frac{U}{V} = \frac{\omega \cdot r}{V},$$

where λ is the tip speed or the peripheral velocity of the rotor, in the case of combined turbine the speed of Darrieus rotor, U is the wind speed, ω is the angular velocity of the rotor, and r is the radius of the rotor.

g) Coefficient of power:

The coefficient of power of a wind turbine (C_P) is the ratio between the maximum power obtained from the wind (P_T) and the total power available from the wind (P_a):

$$C_P = \frac{P_T}{P_a} = \frac{P_T}{(1/2)\,\rho A V^3},$$

where P_T is the power of turbine that is given by

$$P_T = T \cdot \omega.$$

h) Coefficient of torque:

The coefficient of torque or C_T is defined as the ratio between the actual torque developed by the rotor (T) and the theoretical torque available in the wind as expressed by

$$C_T = \frac{T}{T_W} = \frac{4 \cdot T}{\rho \cdot A \cdot d \cdot V^2}$$

$$\text{or } C_T = \frac{C_P}{\lambda},$$

where ρ is the density of air, T is the torque, and A is the swept area of blades = the rotor height × the rotor diameter.

CHAPTER 3: METHODOLOGY

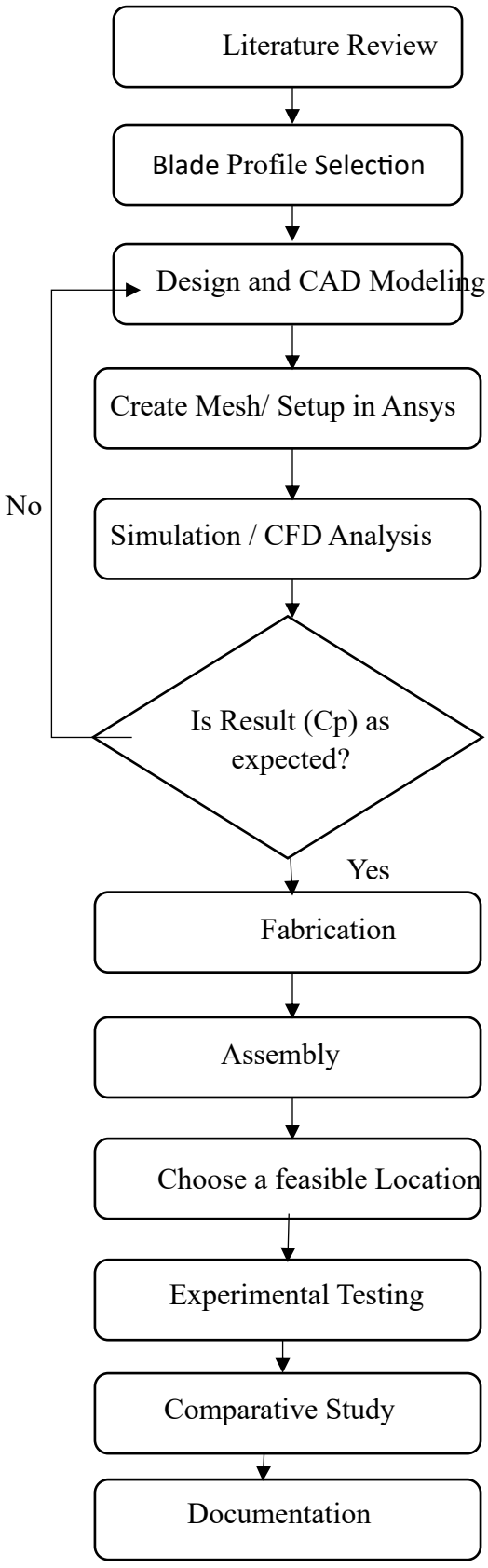

Figure 3.1 : Flow chart of Methodology

3.1 Blade Profile Selection

A comparison between the helical geometry and the conventional Savonius rotor i.e. S-shaped reveals that the helical design performs better. It is observed that the coefficient of power can be improved from 0.12-0.18 to 0.52 with the improvements in Blade shape, i.e. Helical blade. The helical turbine performing slightly better in terms of maximum power coefficient, 9.4% higher in experimental comparison. The helical turbine demonstrated better performance and stability in torque generation when manufacturing complexity is not a concern [1]. The use of both upper and lower circular end plates leads to a significant 36% increase in the power coefficient compared to no end plate [4]. That's why we have taken helical Savonius blade with end plates for our study.

Figure 3.2 Conventional S-shaped Savonius rotor

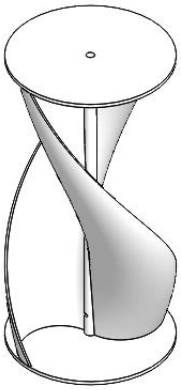

Figure 3.3 Helical Savonius rotor

Similarly, The S- 1046 airfoil has been found to be the optimal choice for achieving higher efficiency, specifically in terms of power coefficient, compared to the standard NACA 0018 airfoil commonly used in previous designs of Darrieus turbines. This means that using the S-1046 airfoil results in a relative increase in power coefficient of about 26.83% [10].

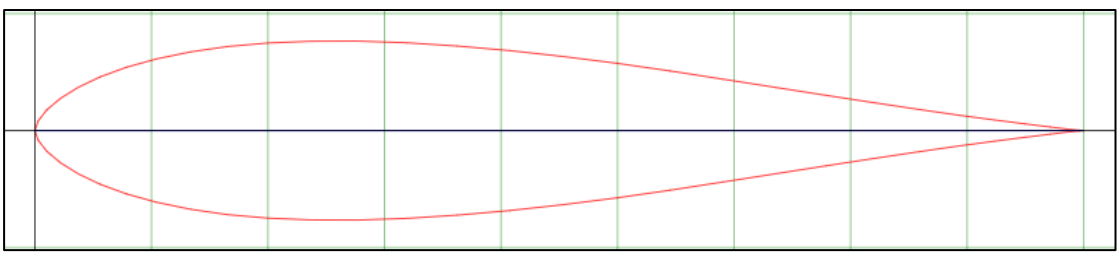

Figure 3.4 S-1046 airfoil shape

3.2 Design and CAD Modeling

Using SolidWorks software, a hybrid VAWT design is developed, integrating both the Helical Savonius and Darrieus configurations as shown in fig 3.4. The S-1046 airfoil coordinates excel file was downloaded from http://airfoiltools.com and was imported into the SolidWorks and extruded to make the Darrieus blade. On the other hand, the Savonius rotor was made using sketch and sweep feature. The 3mm thickness of the Savonius blade is taken as a reference from [15] in which it is 3d printed using PLA filament for experimental testing

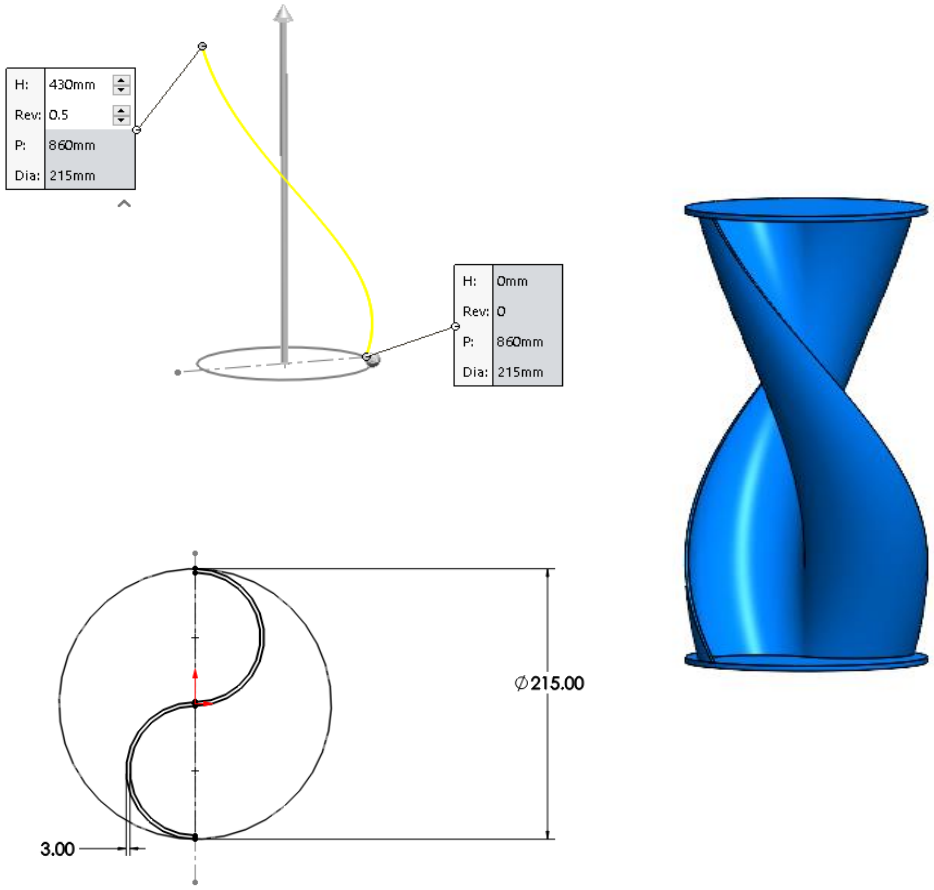

Figure 3.5 Helical Savonius rotor

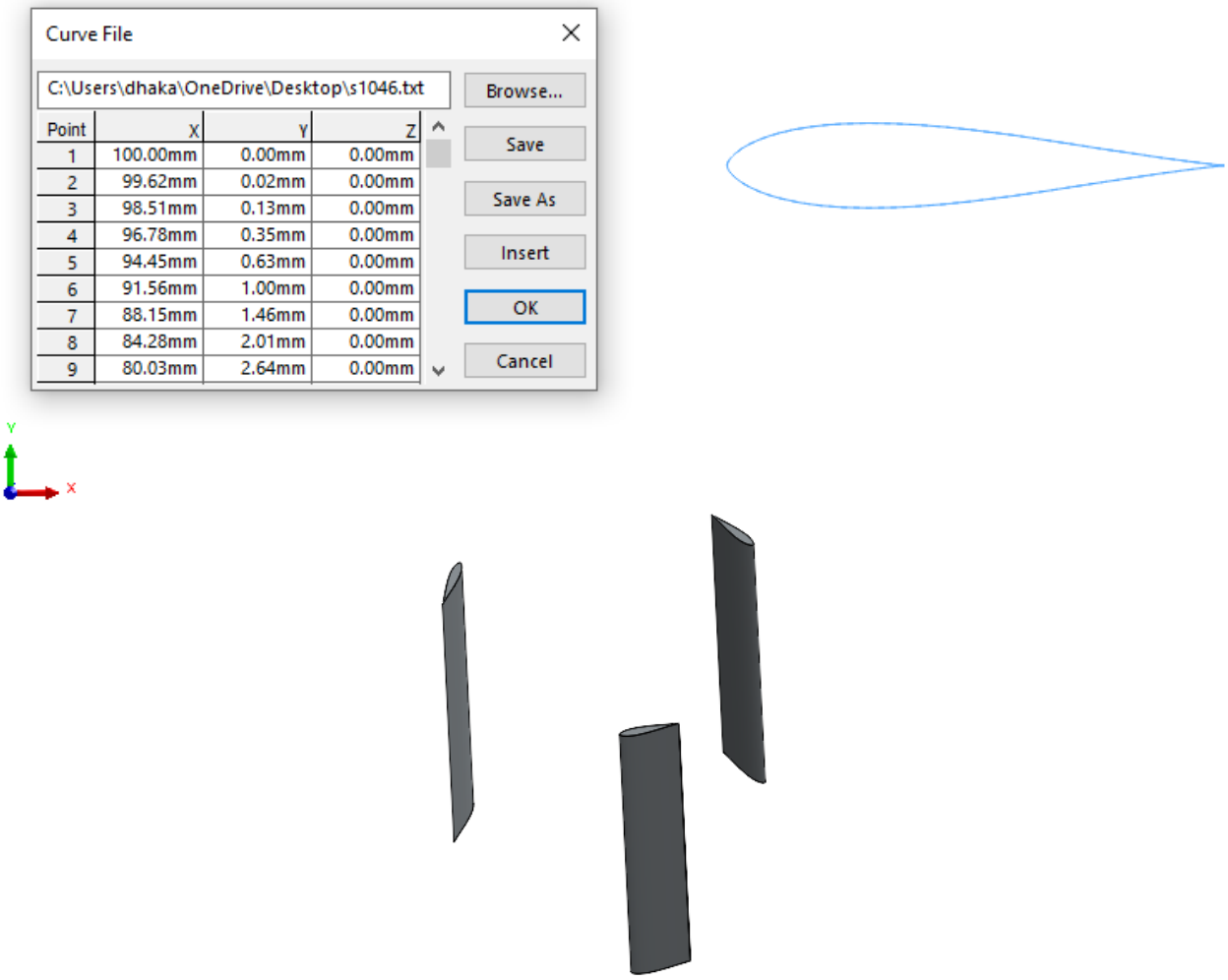

Figure 3.6 Darrieus rotor

These two Helical Savonius and Darrieus blades were combined to form Hybrid rotor as shown below.

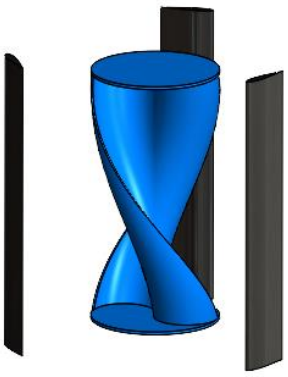

Figure 3.7 Hybrid rotor

3.3 CFD Analysis

ANSYS Fluent 2020 is used to perform CFD analysis. The SolidWorks file is imported into the Ansys design modeler and the two sub domains i.e. rotating and stationary are created. Firstly, to find the optimum radius ratio that gives the highest Coefficient of power, a parametric study is carried out. With the help of the parameter interface shown in fig 3.9 we can easily give different radius of the Savonius rotor while the diameter of the Darrieus rotor is fixed at 500mm. For radius ratios 0.3, 0.33,0.38,0.43 and 0.5, the diameters of Savonius are set as 150mm, 165mm, 190mm, 215mm and 250mm as shown in fig 3.9. Then the meshing is carried out. The figure 3.11 and section 4.1.2 shows the meshing details used. The details about Setup and boundary conditions are discussed in section 4.1.2. Then with the help of Cm and TSR, Cp is calculated and plotted. We can use the option update all design points of the parameter interface which will perform the simulations for different radius ratios one after another.

In our study, radius ratio 0.43 gave the optimum performance. Using that radius ratio, the final Savonius diameter is calculated and the simulations are carried out for solo Darrieus and solo Savonius rotor. Finally, the results are plotted and compared as shown in section 4.1.2.

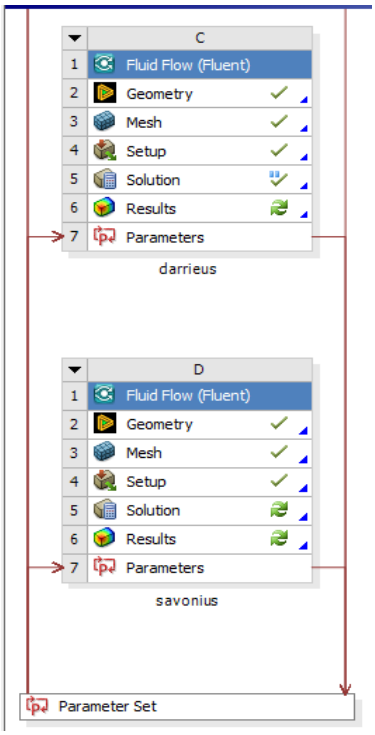

Figure 3.8 Fluent interface

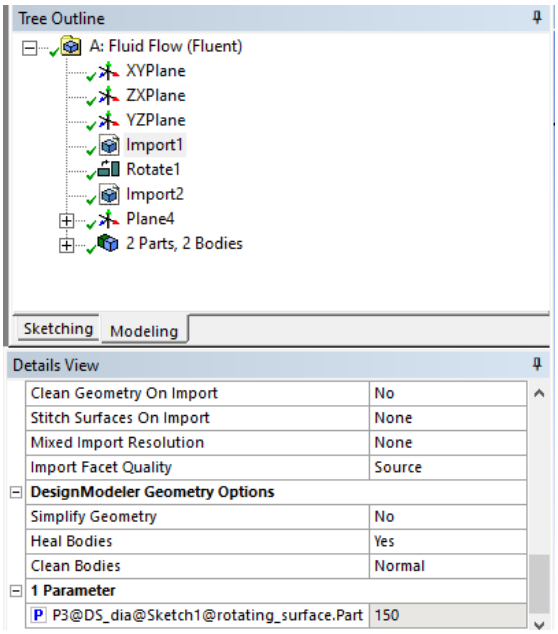

Figure 3.9 Savonius diameter as input parameter

Table of Design Points			
	A	B	H
1	Name	P1 - P3@DS_dia@Sketch1@rotating_sur... .Part	P4 - momentcoeff-op
2	Units		
3	DP 0 (Current)	150	0.046205
4	DP 1	165	-0.030341
5	DP 2	190	-0.030341
6	DP 3	215	-0.030341
7	DP 4	250	-0.030341
*			

Figure 3.10 Parameter set interface

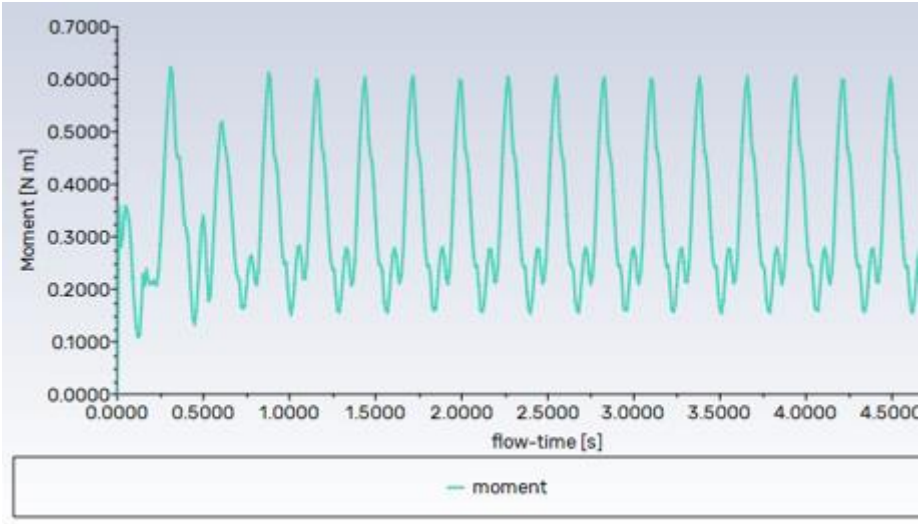

Figure 3.11 Moment over flow time

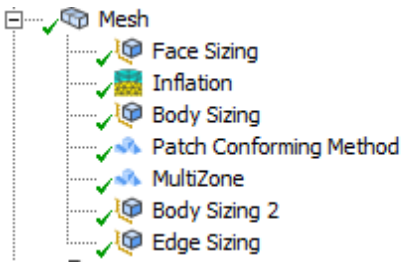

Suppressed	No
Boundary Scoping Method	Named Selections
Boundary	rotor
Inflation Option	First Layer Thickness
First Layer Height	0.26623 mm
Maximum Layers	10
Growth Rate	1.2

Mesh Metric	Orthogonal ...
Min	0.12409
Max	1.
Average	0.98275
Standard Deviation	4.3537e-002

Mesh Metric	Element Quality
Min	0.11262
Max	0.99947
Average	0.92044
Standard Deviation	0.1335

Figure 3.12 Mesh details

3.4 Prototype Development

This section provides a comprehensive overview of the critical steps involved in transforming optimized designs into tangible components. It is really important to pay close attention to every detail and follow exact fabrication methods to make sure the wind turbine is strong and works well. The fabrication process encompassed several key steps which includes material selection, blade fabrication, hub and shaft fabrication, generator assembly, support structure construction etc.

3.4.1 Blade Fabrication

a) Helical Savonius rotor

The helical Savonius rotor was created utilizing 3D printing technology, with the material of choice being PLA (polylactic acid) filament. PLA produces high-quality prints with smooth surfaces and fine details. It has good layer adhesion, which helps prevent delamination and produces strong, durable prints [20]. It is generally more affordable compared to some other filaments such as ABS or nylon. This makes it a cost-effective option for 3D printing projects, especially for small-scale production [21]. The 3d printed Savonius rotor had a volume of 586.62 cm^3 and the density of 1.25g/cm^3.

Figure 3.13 3d printed Savonius rotor

b) Darrieus Rotor blades

The making of Darrieus rotor blades involving the fabrication of ribs supported by carbon fibers support and laminating them with flex tapes. Flex Tape is a type of adhesive tape commercially available and known for its strong and

flexible properties [22]. It is made of a durable, waterproof backing material coated with a rubberized adhesive. Flex tape is easy to use and cost-effective making it convenient and reliable option for this project.

The ribs for the Darrieus rotor blades were crafted using laser cutting technology, employing 9 mm thick plywood panels. Laser cutting allowed for precise shaping of the S-1046 profile onto the plywood, along with the necessary support tube aperture. the carbon fiber tube with a square cross-section and sides measuring 8 mm in length is used to serve as the support tube. Carbon fiber is renowned for its outstanding strength-to-weight ratio, rendering it considerably lighter than conventional materials such as steel while retaining excellent strength properties [22]. As a result, the vertical axis wind turbine (VAWT) benefits from a reduced overall weight, potentially alleviating structural stress and improving portability during the installation process.

A set of three Darrieus blades were constructed, each consisting of 24 ribs of aero foil profile affixed to the support tube at uniform intervals along its length using a glue gun. Following this, the structure underwent two rounds of lamination with Flex Tape, resulting in the complete structure of the Darrieus blade.

Figure 3.14 Ribs of blade profile S-1046

Figure 3.15 Assembled ribs

Figure 3.16 Darrieus blade

3.4.2 Shaft and Holder

A 1-meter-long mild steel rod with a diameter of 12mm serves as the rotor shaft. Three 3mm holes are drilled into the rotor at distinct positions to secure the Savonius blade onto the rotor shaft. Each of the three Darrieus rotors is affixed to the rotor shaft via a hub arrangement.

This arrangement comprises two 3D-printed support fastened to the rotor shaft, with six aluminum tubes which acts as a support connecting the Darrieus blades to the shaft via 3d printed holder.

Figure 3.17 3D printed Darrieus holder

Figure 3.18 Assembly of Darrieus blades to shaft

3.4.3 Dynamo assembly

The dynamo assembly features a sturdy frame to which the dynamo is securely affixed using screws. It is linked to the rotor shaft via two gears with a module of 1.5. These gears were fabricated by 3d printing technology using PLA filament. Both the gears were provided with gear bush having 23 mm external diameter and 10 mm height. Gear for rotor shaft was given 13mm of internal diameter hole and key-slot was made in gear for dynamo shaft for coupling with dynamo. The gear connected to the rotor shaft contains 40 teeth, while the complementary gear connected to the dynamo boasts 20 teeth. Consequently, the gear assembly achieves a gear ratio of 2, indicating that the angular velocity of the dynamo is twice that of the rotor shaft.

Figure 3.19 Gear for rotor shaft

Figure 3.20 Gear for dynamo shaft

3.4.4 Support structure construction and assembly

The support structure comprises a rigid framework upon which the entire vertical axis wind turbine is mounted and supported, with its height adjustable to accommodate the specific elevation of the wind tunnel during testing. The rigid frame consists of four steel tubes, each with a square cross-section measuring one inch on each side, fastened together to create a square frame of cross section 77.4 cm x 67.4 cm. Pillow block bearings are affixed to the top and bottom steel rods of the frame to support the rotor shaft, allowing it to rotate freely. A separate platform welded onto the frame holds the dynamo securely with screws, while the dynamo shaft is connected to the turbine rotor via a gear coupling.

Figure 3.21 Pillow block bearing

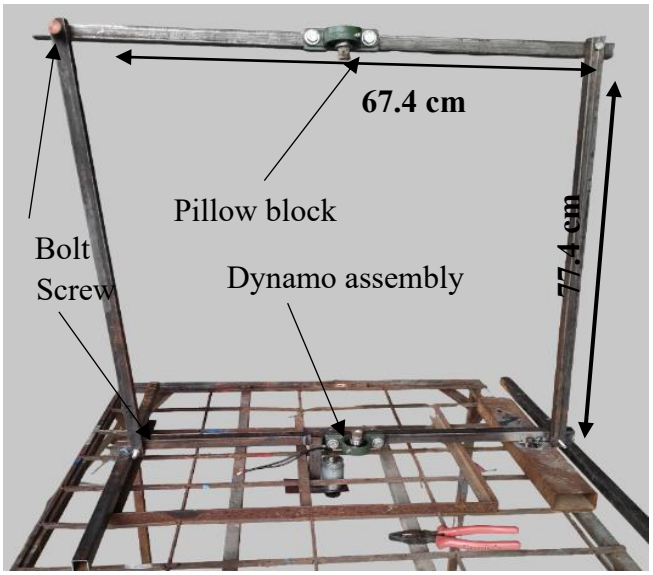

Figure 3.22 frame support for VAWT

3.5 Experimental Testing

A comprehensive experimental testing phase was conducted to evaluate the performance of the prototype.

3.5.1 Wind Tunnel

A wind tunnel is a machine used in aerodynamics and fluid mechanics to study the effects of airflow around objects. It consists of a long, enclosed tube with a fan or other means of generating airflow at one end. The object or model to be tested is placed inside the tunnel, and air is forced to flow over or around it at controlled speeds [23].

In this present work, the experimental testing was conducted at National Innovation Centre (NIC), Kirtipur. The wind tunnel at NIC features a larger test section with dimensions of 60×60 cm^2. Further, the wind speed can be varied from around 4 m/s up to 30 m/s making it suitable for testing over wide range of speed.

Figure 3.23 Wind tunnel

a) Impeller Section

The impeller section of a wind tunnel is a critical component responsible for generating airflow within the tunnel. Typically located at one end of the tunnel, the impeller consists of a set of rotating blades or fans driven by a powerful motor. As the impeller rotates, it draws in air from the surrounding environment and accelerates it to create a controlled airflow through the tunnel. The design and configuration of the impeller are essential for ensuring uniform airflow velocity and direction throughout the test section of the wind tunnel. Additionally, the impeller section may include features such as diffusers and screens to streamline airflow and minimize turbulence[23].

Diameter of the impeller Section: 4 feet

Figure 3.24 Impeller section

b) Test Section

The test section of a wind tunnel is the portion where models or objects are placed to be subjected to airflow for aerodynamic testing. It's the part of the wind tunnel where experiments are conducted and data are collected. The test section is typically located downstream of the impeller section where airflow is generated. It's designed to have a uniform, stable airflow with controlled conditions, allowing researchers and engineers to accurately measure the aerodynamic forces and moments acting on the models being tested[23]. External anemometer was inserted inside the test section for measuring the wind speed in that section. The features of the used wind tunnel's test section are:

Cross section of the square test section: 60 cm x 60 cm

Length of the section: 120 cm

Figure 3.25 Test section

c) Air intake section

The air intake section of a wind tunnel serves as the entry point for airflow into the testing environment. Positioned at the front end of the tunnel, it comprises carefully designed openings or ducts that allow atmospheric air to be drawn into the tunnel system. The configuration of the air intake section is crucial for ensuring a uniform and controlled airflow throughout the tunnel, minimizing disturbances and turbulence. Various features such as screens, filters, and

diffusers may be incorporated into the intake section to regulate airflow quality and direction as shown in Figure 3.25.

Intake Section Dimension: 6.3ft x 6.3ft

Figure 3.26 Inlet section

d) Wind tunnel dimension:

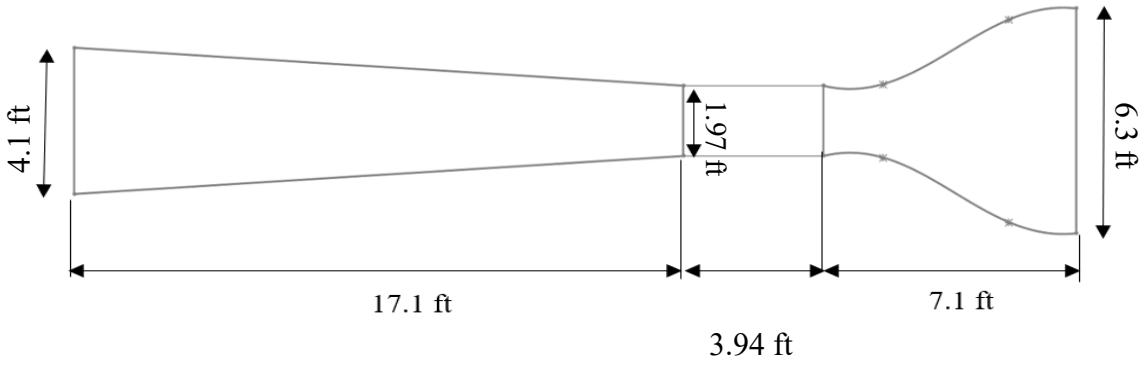

Figure 3.27 Wind tunnel dimensions

3.5.2 Measuring Devices

a) Tachometer

In wind tunnel testing for wind turbines, a tachometer serves as a fundamental tool for monitoring rotor speed. It measures the revolutions per minute (RPM) of the turbine blades, providing essential data for engineers to analyze the

performance and aerodynamics of the turbine under simulated wind conditions. By accurately tracking rotor speed, factors such as efficiency and power output can be accessed.

Specification of used tachometer:

- Micro digital
- Measures 2 to 9 propellers.
- 0-99999rpm range

Figure 3.28 Tachometer

b) Anemometer

In wind tunnel testing, an anemometer was used to measure the velocity of the wind in the test section. Based on the output of anemometer, the wind speed was varied increasingly. The anemometer used in the experiment was a Pitot tube anemometer and differential manometer. It includes a Pitot tube and 2 connection hoses for measuring Air Velocity/Air Flow. It can measure the air velocity ranging from 200 ft/min to 15733 ft/min

Figure 3.29 Anemometer

c) DC motor generator

A DC motor generator converts mechanical energy to electrical energy via electromagnetic induction. In wind turbine applications, it plays a crucial role by converting the turbine's rotational energy into electricity. This electricity powers various components or is stored for later use. Known for their stable voltage output, DC motor generators ensure a reliable power supply from wind turbines. With a simple yet robust design, they are well-suited for the demanding conditions of wind energy production.

Specs of the DC motor Generator Rated voltage: 12V

Rated power: 50 W

RPM: 2000 rpm

Figure 3.30 DC motor

d) Multimeter

In wind tunnel testing, the multimeter was used to assess the electrical performance of the turbine's generator system. By connecting the multimeter to the DC motor, both current and voltage generated by the turbine under simulated wind conditions was measured. These measurements provide essential data for calculating the power output of the turbine.

Voltage measurement: The multimeter was used to measure the voltage output of the turbine's generator. This measurement indicates the electrical potential difference generated by the rotating turbine blades as they interact with the airflow in the wind tunnel.

Current measurement: The electrical current flowing through the DC motor connected to the turbine's generator was measured. This measurement represents the rate of flow of electrical charge and indicates the amount of power being transferred from the turbine to the motor.

Power calculation: Once voltage and current measurements are obtained, the electrical power generated by the turbine was calculated using the formula:

Power (P) = Voltage (V) × Current (I).

Figure 3.31 Anemometer

e) Speed Control

At the Wind Tunnel section of the National Innovation Centre, a frequency-based speed controller readily available to regulate the impeller speed was utilized during the wind turbine testing. With the guidance from senior operator helped to understand the operation of the controller. The frequency could be easily adjusted to control the impeller speed. Setting the frequency to a minimum of 14 Hz resulted in a wind speed of approximately 3.5 m/s in the test section of the tunnel. In contrast, setting the frequency to 29 Hz allowed to achieve a wind speed of about 12 m/s. This setup enabled precise control over the wind turbine's impeller speed, facilitating comprehensive testing across a range of wind conditions.

Figure 3.32 Speed controller

3.5.3 Experimental Setup

a) Savonius Rotor

The experimental setup for the Savonius turbine utilized a pre-fabricated frame from the workshop to support the turbine shaft. A lower stand was constructed from available metal scraps at the National Innovation Centre (NIC). Upon assembly of the upper frame onto the lower stand, the dynamo and gear assembly were installed. Subsequently, the Savonius rotor was inserted through the shaft via the upper opening section of the test apparatus and secured to the shaft using screws. Regulation of impeller speed was achieved using a speed controller, while wind speed within the test section was measured using an anemometer equipped with a pitot tube. Additionally, the RPM of the shaft, driven by the Savonius blades, was recorded using an infrared tachometer. Voltage and current were measured using a multimeter connected to the DC motor to further analyze the turbine's performance. This comprehensive setup facilitated the efficient conduct of the experiment.

Figure 3.33 Savonius rotor

Specifically, for the Savonius turbine, wind speed ranged from 3.438 to 9.326 m/s. The minimum recorded turbine speed during the lowest wind speed was 109.86 rpm, while the maximum speed reached 672.984 rpm.

b) Darrieus Rotor

Upon completion of data collection for the Savonius rotor, the setup was disassembled from the upper section, and subsequently, the Darrieus rotor was installed in the test section. Employing identical parameters and procedures as previously described, data acquisition commenced. However, at an initial wind

speed of 3.561 m/s, the Darrieus turbine remained motionless. Rotation of the turbine commenced only when the wind speed was increased to 7.937 m/s, at which point the minimum recorded speed was 150.254 rpm. As wind speed further increased to 10.895 m/s, the turbine attained its peak rotational speed of 865.456 rpm. This meticulous data collection process facilitated a comprehensive analysis of the Darrieus turbine's performance across varying wind speeds, thereby providing valuable insights into its operational characteristics and efficiency.

c) Hybrid Rotor

Following the completion of data collection for the individual turbines, the setup was once more disassembled and both the Savonius and Darrieus rotors were fitted inside the shaft through the upper section of the test section, utilizing a similar setup as before. Upon integration, the Hybrid rotor started rotation at a minimum wind speed of 4.425 m/s. At this speed, the turbine exhibited a speed of 75.632 rpm. As wind speed reached to 10.863 m/s, the combined turbine reached its maximum speed, reported at 852.166 rpm. This amalgamation of turbine designs provided valuable data on the performance of the hybrid configuration, showcasing its ability to start rotating at lower wind speeds and achieve efficient operation at higher wind speeds.

Figure 3.35 Hybrid rotor

3.6 Comparative Analysis

The results obtained from experimental testing were recorded, and a comparative analysis was conducted between the data acquired from the hybrid rotor and those from the individual rotors. This comparative assessment is elaborated upon in Section 4.3

3.7 Documentation

Finally, documentation of the overall project is carried out.

CHAPTER 4: RESULTS AND DISCUSSION

4.1 CFD Analysis

a) Geometry:

In this investigation, rotor performance is evaluated using a finite volume approach in a three-dimensional rectangular flow domain, as depicted in Fig.4.3. The domain consists of two sub-domains: a rotating circular zone containing both Darrieus and Savonius rotors, and a stationary zone surrounding the rotating zone. The computational domain has dimensions of 15D in the streamwise direction and 8D in both vertical and lateral direction, where "D" represents the external rotor diameter. To ensure accuracy and avoid boundary effects, the domain size is selected to be sufficiently large based on previous studies [16].

The rotating zone, where the hybrid rotor operates counterclockwise, has a diameter of 1.5D. The center of the hybrid rotor is positioned 5D from the inlet and 4D from both upper and lower boundaries, with the coordinate origin at the rotor's center. Similarly, the specifications of the proposed turbine are shown in Table 4.1.

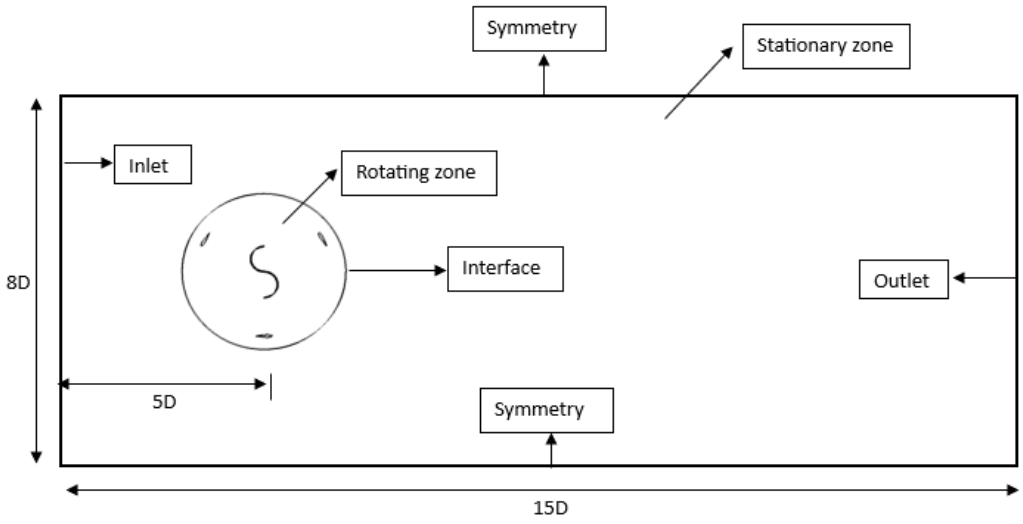

Figure 4.1 Computational Domain

Figure 4.2 Hybrid rotor imported to Ansys Geometry

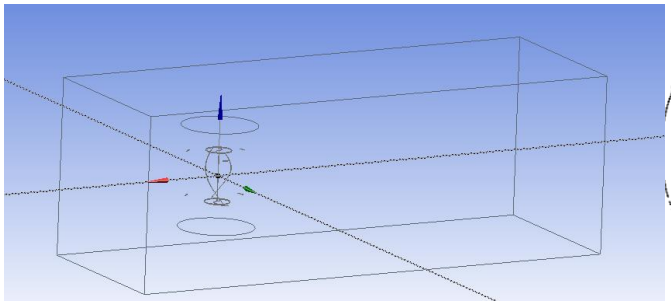

Figure 4.3 3D computational domain

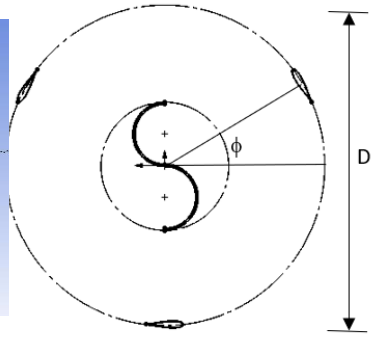

Figure 4.4 Section view

:

Table 4.1 Characteristics of suggested Savonius and Darrieus blades

Parameter	Savonius Blade	Darrieus Blade
Rotor Diameter, mm	Ds= 215	D= 500
Rotor Height, mm	Hs= 430	H= 500
Aspect Ratio, AR	2.0	1.0
Non-dimensional Chord length	-	0.18
Chord length, mm	-	90
Attachment angle (ϕ)	-	30°

b) Meshing:

Since unstructured mesh can handle curvature boundaries of arbitrary shape, it was used. Similarly Quadrilateral Dominant meshing was used as it is an efficient method compared to Triangular for compact meshing. The stationary domain's body mesh size is three times that of the rotating zone, with a finer grid employed in the boundary layer on the rotor surface (comprising Savonius and Darrieus blades) to enhance the flow field near the wall. In this numerical investigation, 10 prism layers are utilized near the wall of both Savonius and Darrieus blades, where the first layer has a height of 0.26623 mm and a growth rate of 1.2. This ensures a maximum dimensionless wall distance (y+) of less than 5 over both blade types.

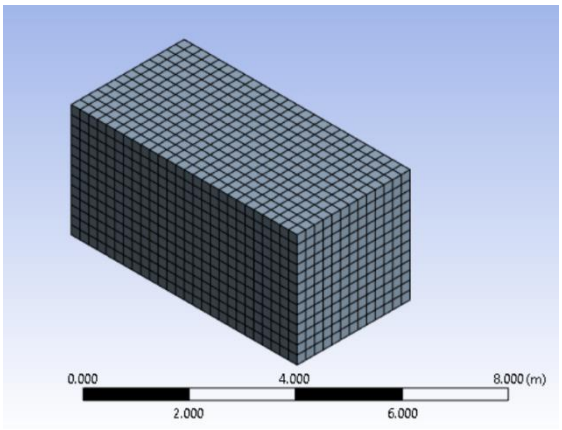

Figure 4.5 Mesh of 3D model

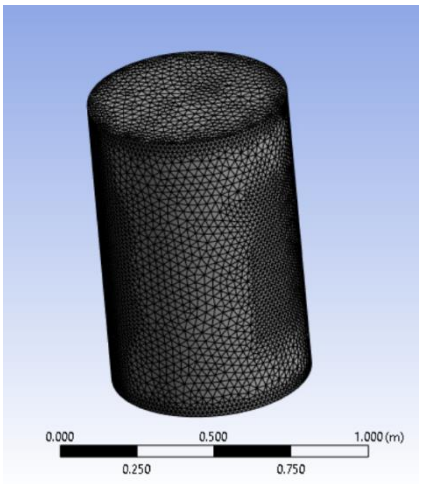

Figure 4.6 Mesh of rotating zone

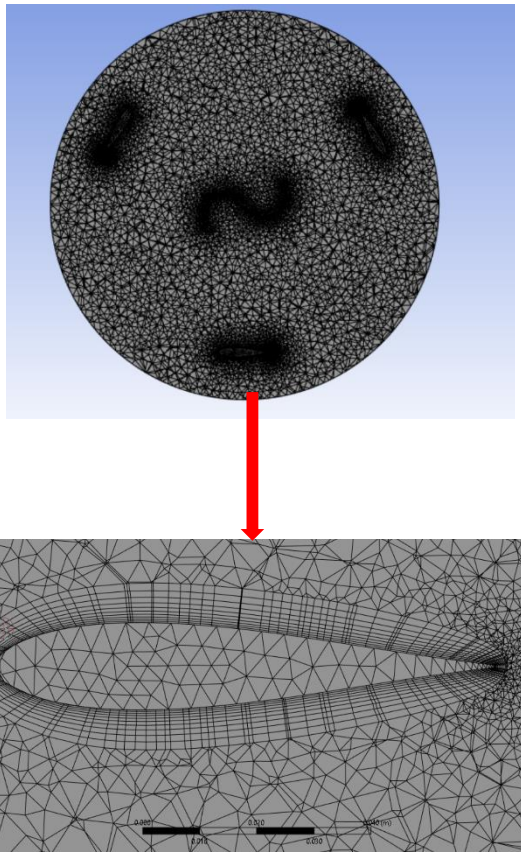

Figure 4.7 Sectioned View

By averaging the results of the last cycle, torque coefficient is calculated. To ensure numerical accuracy, a mesh

Table 4.2 Details of refinement levels

independence study was carried out on a specific design with a radius ratio of 0.3. This investigation aimed to assess the impact of varying the number of nodes and elements on the solution. Both sides of the interface boundary conditions were meshed with a similar number of elements to expedite convergence, particularly concerning the continuity equation. The density and quality of unstructured grids in a three-dimensional domain were investigated and scanned across various grid sizes, ranging approximately from 750,000 to 1,000,000 cells. The analysis revealed that using over 980,000 cells resulted in torque coefficient deviations of less than 1.36%. Consequently, a grid size of 982,940 cells was kept for all computations to minimize computational time.

Refinement Level	No. of Nodes	No. of Elements	Cm
1	756168	3056049	0.143004
2	854465	3327605	0.14413
3	982940	3737181	0.150613
4	993621	4313701	0.152702

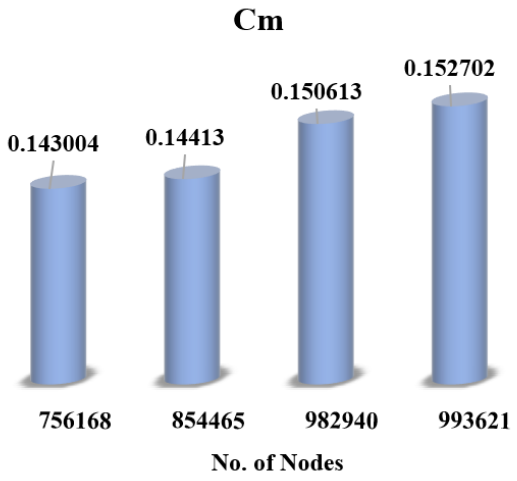

Figure 4.8 Mesh of 3D model

c) Setup

Turbulence modeling:

Menter [6] introduced the k-ω SST model to integrate the accurate and robust formulation of the k-ω model with the k-ε model. This integration aims to capitalize on the strengths of the k-ω model in regions near the wall, as it provides precise results in those areas, while the k-ε model is effective in regions farther from the wall where free flow is significant. The k-ω SST model demonstrates notable proficiency in both low and high Reynolds number regions, combining the advantageous features of the k-ω model in low Reynolds number areas and the appropriate characteristics of the k-ε model in high Reynolds number regions. Recent investigations into turbulent flow modeling around vertical- and horizontal-axis wind turbines, as well as simulations of flow around aerators employed in wind turbines, indicate that the k-ω SST model consistently yields acceptable and satisfactory solutions. The formulated transport equations for turbulence kinetic energy (k) and specific dissipation (ω) in the SST k-ω model are as follows:

$$\rho\frac{d}{dt}(k)+\rho\nabla.\left[k(\vec{u}-\vec{u}_g)\right]=\nabla.\left[\left(\mu+\frac{\mu_t}{\sigma_k}\right)\nabla k\right]+G_k-Y_k$$

$$\rho\frac{d}{dt}(\omega)+\rho\nabla.\left[\omega(\vec{u}-\vec{u}_g)\right]=\nabla.\left[\left(\mu+\frac{\mu_t}{\sigma_\omega}\right)\nabla\omega\right]+G_\omega-Y_\omega$$

Boundary conditions and solver details:

The ANSYS Fluent software, a commercially valuable Computational Fluid Dynamics (CFD) tool, proves instrumental in modeling fluid flow within intricate geometries. For the wind turbine simulation, a rotating reference frame (Sliding mesh type) is employed, designating the wind turbine as a wall boundary. Table 4.2 provides details on the boundary types for each component of the fluid domain. The far-field aspect of the boundary is set as a free slip wall, while the wind turbine blades are treated as no-slip walls. Boundary Conditions are specified as inlet velocity 6 m/s while the angular velocity is varied. An outlet pressure with a zero value is implemented to eliminate pressure differentials at the outlet. The analysis employs standard air with a density of 1.185 kg/m^3 and a dynamic viscosity of 1.183x10^-5 kg/(ms) at 25°C. The time step size is taken as 0.001 s for all tip speed

ratios as a suitable time for all rotational speeds and computational iterations continue until reaching residuals of 10^-4 for all governing equations.

ANSYS Fluent 20.0, utilizing a pressure-based transient finite volume method solver, discretizes the fluid flow equations. The spatial discretization of conservative equations adopts the 2nd order upwind scheme, and the temporal terms use the 2nd order fully implicit temporal scheme. The pressure–velocity coupling employs the Semi-Implicit Method for Pressure Linked Equations (SIMPLE) algorithm. SIMPLE is an iterative process involving a guess-and-correct approach for pressure calculation. Initially, an imperfect velocity field based on a guessed pressure field is computed, and the continuity equation guides pressure correction. This iterative method accommodates the sequential calculation of other scalars coupled to the momentum equations.

Table 4.3 Boundary Conditions type

Surface	Boundary Conditions type
Inlet	Inlet Velocity
Sides, Top, and Bottom	Symmetry
Outlet	Atmospheric Pressure
Rotor blades	Wall with nonslip condition

d) Result:

1) Performance of hybrid rotors at different radius ratios β:

The power coefficient characteristics of the turbine rotors with different radius ratios are presented in Figure 4.9. As seen in the figure, the maximum power coefficients have been obtained around 0.22145 for β = 0.3, 0.24 for β = 0.33, 0.30246 for β = 0.38, 0.35678 for β = 0.43 and 0.33153 for β = 0.5. The curves show that the highest power coefficient is found for β = 0.43 and afterward i.e. for β = 0.5 the power coefficient decreases. It is because the higher radius ratio increases the interaction between the Savonius and Darrieus blades and hence, the operating range of tip speed ratio is reduced. It is concluded that the higher

the dimension of Savonius bucket is, the higher the losses become; thereby the performance decreases. So, it seems that the optimum condition occurs to β = 0.43. For the better condition in the design of a combined wind turbine, the rotor should have a self-starting point at low speed, a high torque operation, a high speed, and a high-power coefficient. So, it is suggested to use the radius ratio 0.43 in the design of a combined turbine.

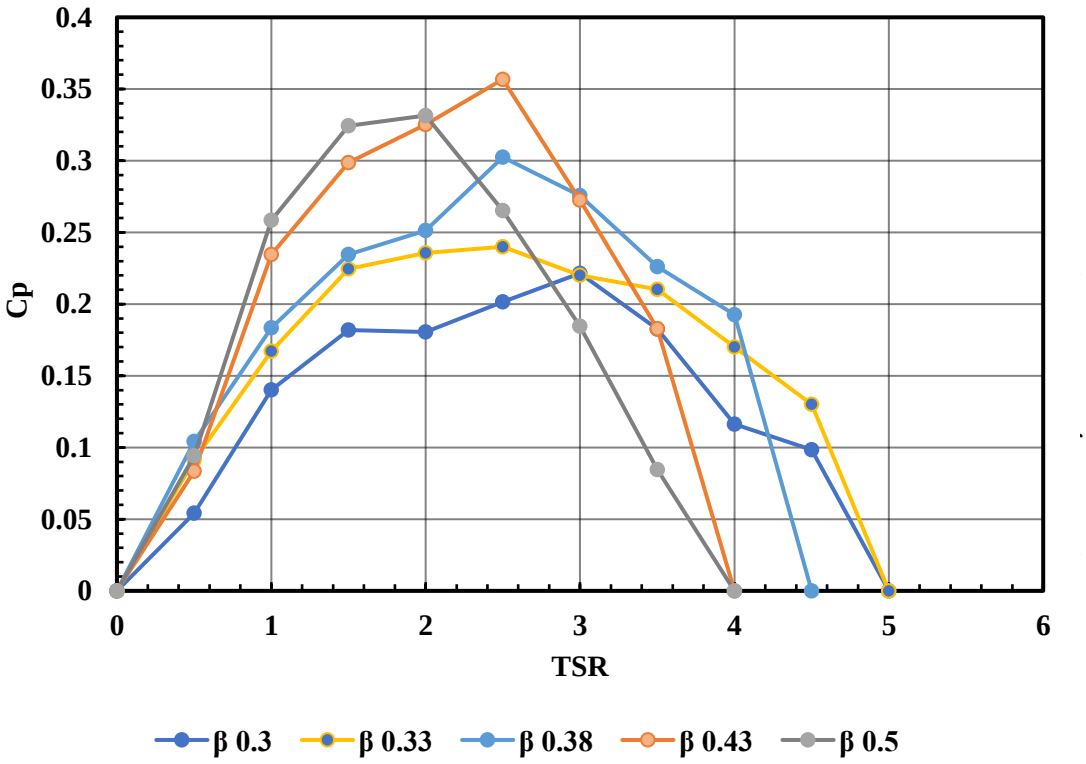

Figure 4.9 Cp vs TSR at different radius ratios

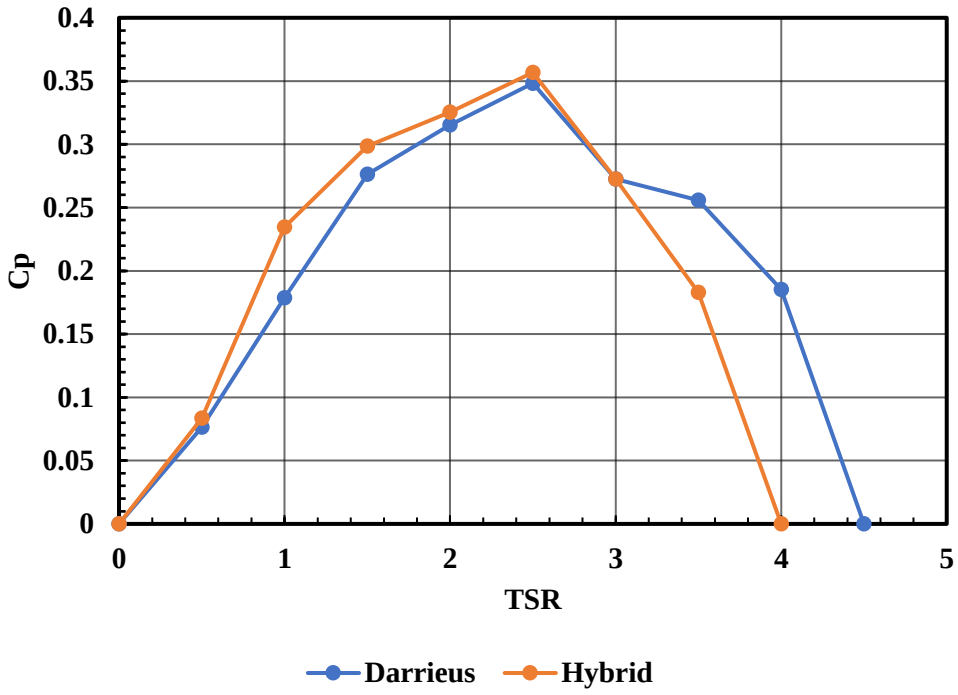

Figure 4.10 Cp vs TSR of hybrid rotors at radius ratio β = 0.43 compared with Darrieus rotor

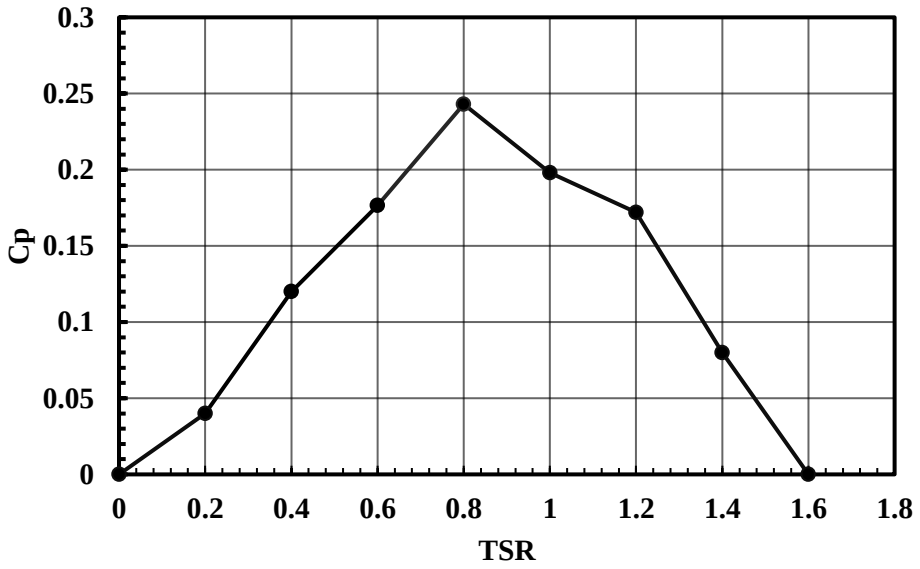

Figure 4.11 Cp vs TSR of Solo Savonius rotor

But on the other hand, Fig.4.11 shows that Savonius rotor operates over a very small TSR range which makes it suitable for low-speed applications. The maximum power coefficient achieved is 0.2498 at $\lambda = 0.8$ which is quite low compared to Cp= 0.35678 of Hybrid rotor. Thus, we can conclude that Hybrid rotor helps to harvest more wind energy and can operate at higher speeds.

3) Self-Starting Ability of Rotors:

In Fig 4.12, the coefficient of moment of Solo Darrieus rotor and Hybrid rotor is plotted against wind speed. In this study the velocity of wind was varied from 1 to 5 m/s and the objective was to check the starting ability of these rotors. From the figure we can see that coefficient of moment is quite high for hybrid rotor at low wind speed making it capable of starting at low wind speed. On the other hand, Darrieus rotor should be provided with initial rotation by some mechanism so that it begins to rotate.

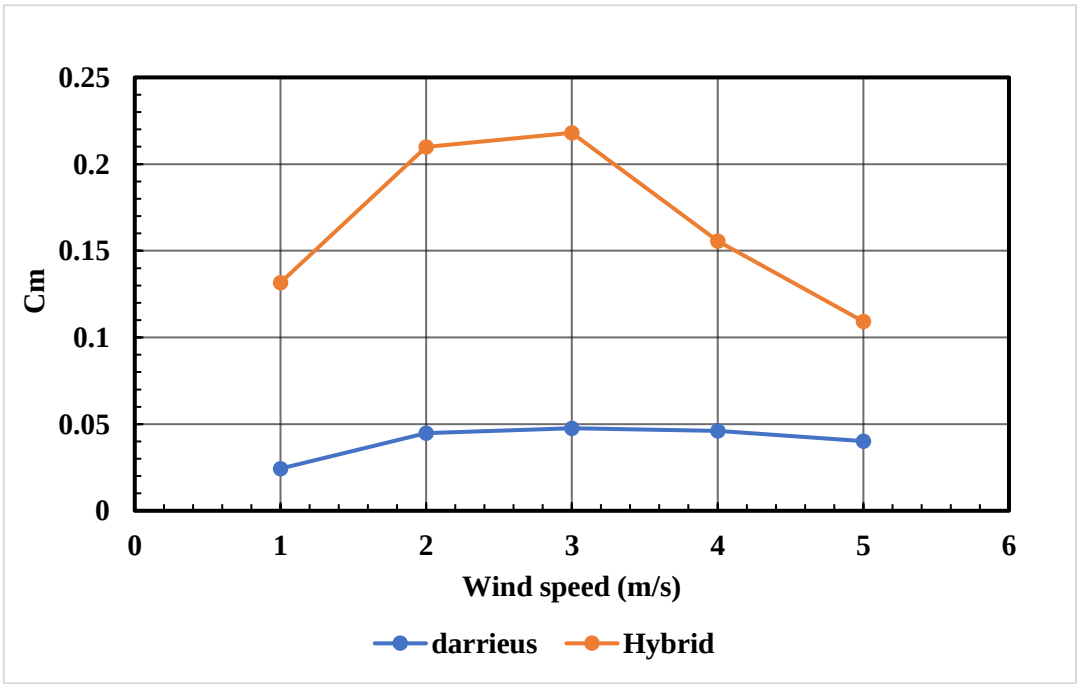

Figure 4.12 Cm vs wind Speed of Hybrid rotor compared with Darrieus rotor

4.2 CAD Model

The design of Savonius and Darrieus rotor blades with all the necessary components of the turbine was designed based on SOLIDWORKS. The detailed drawing sheet of the CAD model is shown in appendix. The isometric and side view of the designed model is shown below:

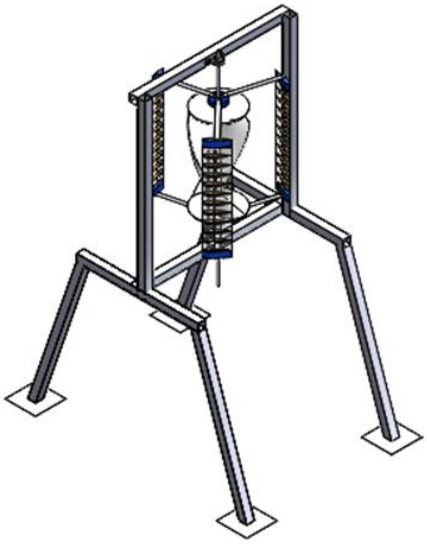

Figure 4.13 Isometric View

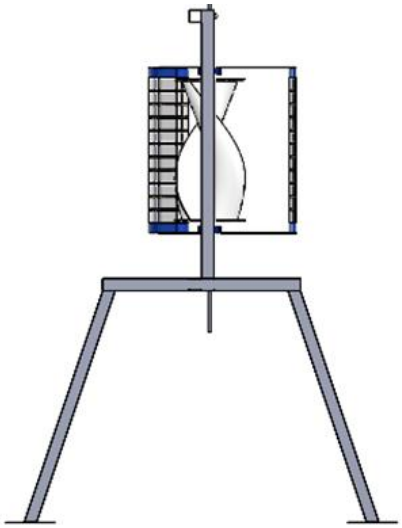

Figure 4.14 Side view

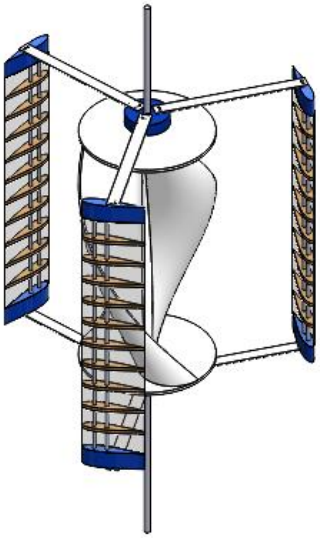

Figure 4.15 Combined rotor

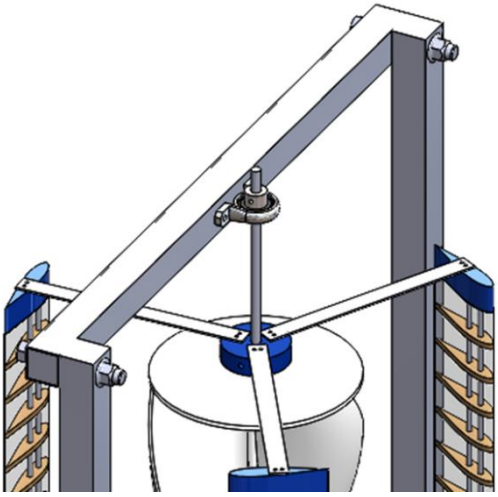

Figure 4.16 Cropped Isometric View

4.3 Experimental Testing

a) Results and Discussion of Savonius Turbine

Table 4.4 Performance Coefficient of fabricated model of Savonius rotor

Experiment	Wind velocity (m/s)	rpm	Voltage (V)	Current (A)	Power Exp. (W)	Power Th. (W)	Torque Exp. (Nm)	Cp	TSR
1	3.438	109.86	0.211	0.081	0.017	2.262	0.001	0.756%	0.360
2	4.761	162.356	1.203	0.275	0.331	6.006	0.019	5.508%	0.384
3	5.432	201.34	1.426	0.623	0.888	8.920	0.042	9.959%	0.417
4	6.106	255.125	1.913	0.755	1.444	12.670	0.054	11.400%	0.470
5	6.424	275.012	2.123	1.022	2.170	14.754	0.075	14.706%	0.482
6	7.105	310.245	2.252	1.612	3.630	19.962	0.112	18.186%	0.492
7	8.096	470.356	3.321	1.651	5.483	29.533	0.111	18.565%	0.654
8	8.372	510.235	3.951	1.813	7.163	32.658	0.134	21.934%	0.686
9	9.326	672.984	4.321	2.092	9.040	45.143	0.128	20.024%	0.812

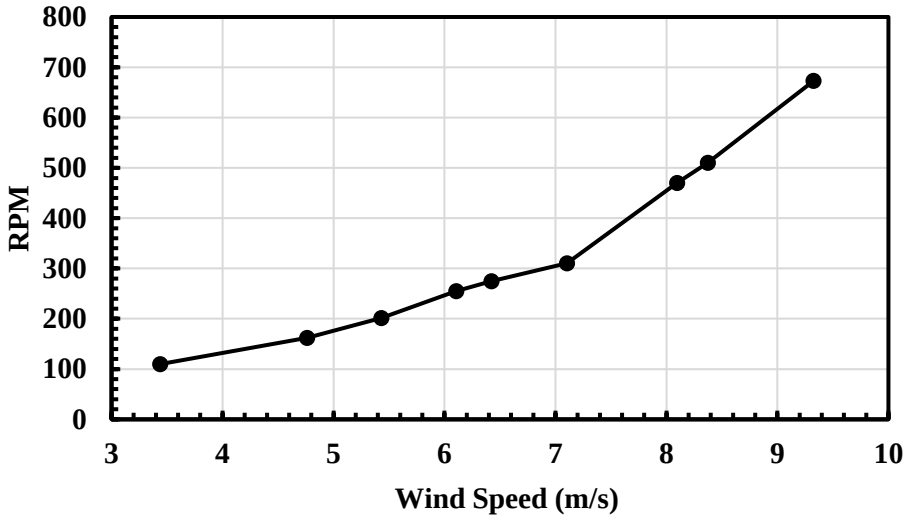

Figure 4.17 Variation of turbine speed with wind speed for Savonius rotor

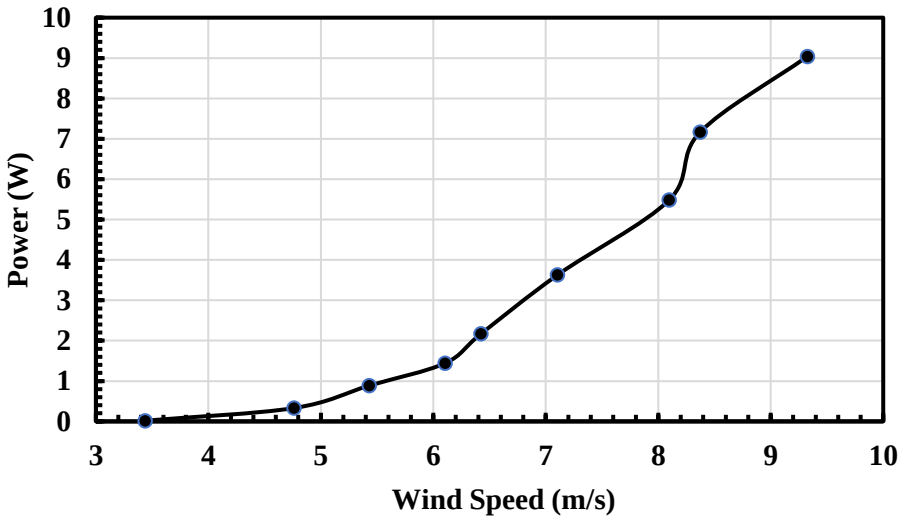

Figure 4.18 Variation of turbine power with wind speed for Savonius rotor

In Figures 4.17 and 4.18, the variation of turbine speed and power with wind speed for Savonius rotor is depicted. Wind speed ranged from 3.438 m/s to 9.326 m/s. The maximum turbine speed recorded was 672.984 rpm at a wind speed of 9.326 m/s. It is noteworthy that the rotor could have started at wind speeds lower than 3.438 m/s, but due to limitations of the wind tunnel, the lowest starting speed achievable was around 3.5 m/s. This limitation underscores the relatively lower self-starting ability of Savonius rotors.

Moreover, Figure 4.18 illustrates that the rotor attained its maximum power output of 9.040 W at a wind speed of 9.326 m/s.

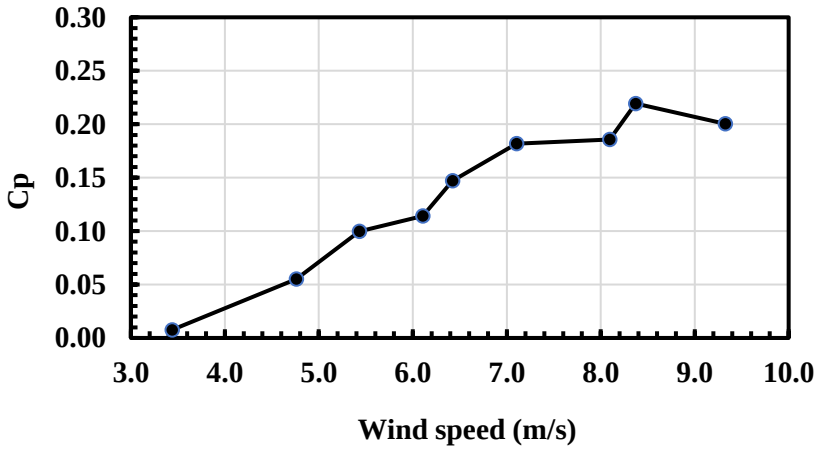

Figure 4.19 Variation of coefficient of power with wind speed for Savonius rotor

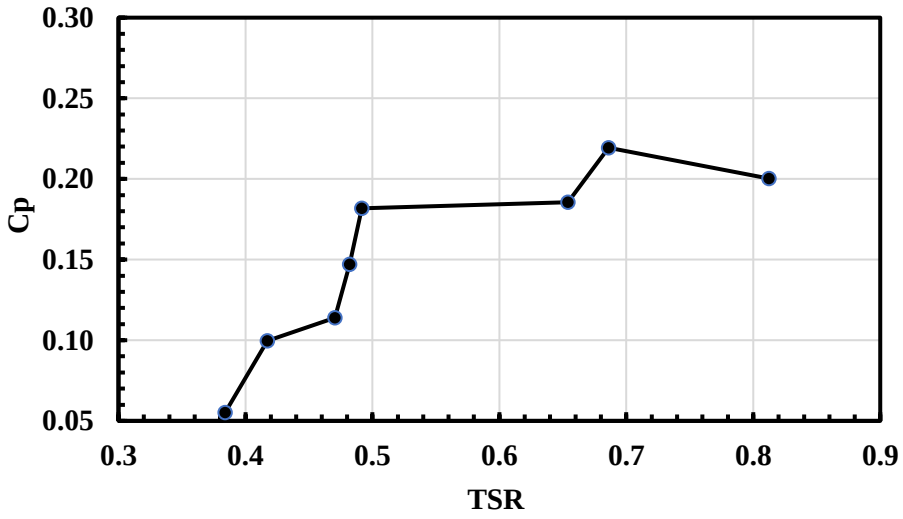

Figure 4.20 Variation of coefficient of power with TSR for Savonius rotor

Figure 4.19 presents the variation of the coefficient of power (Cp) with wind speed. Notably, a maximum Cp of 21.934% was attained at a wind speed of 8.372 m/s and at a wind speed of 9.326 m/s the Cp reduced to 20.024%. Similarly, Figure 4.20 depict the variation of Cp with Tip Speed Ratio (TSR) for the Savonius rotor. It is observed that the TSR range for the Savonius rotor is narrow, indicating suitability for low-speed applications.

The maximum power coefficient achieved is 21.934% at a TSR of 0.686. This value is slightly lower than the 24.98% obtained from Computational Fluid Dynamics (CFD) analysis. However, such disparities are expected due to mechanical losses not accounted for in experimental measurements, particularly in power measurement

b) Results and Discussion of Darrieus Turbine

Table 4.5 Performance Coefficient of fabricated model of Darrieus rotor

Experiment	Wind velocity (m/s)	rpm	Voltage (V)	Current (A)	Power Exp. (W)	Power Th. (W)	Torque Exp. (Nm)	Cp (%)	TSR
1	3.561	-	-	-	-	6.796	-	-	-
2	5.578	-	-	-	-	26.120	-	-	-
3	5.843	-	-	-	-	30.022	-	-	-
4	6.651	-	-	-	-	44.279	-	-	-
5	7.937	150.254	5.896	1.041	6.137	75.250	0.390	8.156%	0.496
6	8.868	290.245	8.215	2.114	17.362	104.958	0.571	16.542%	0.857
7	9.941	509.768	8.625	3.925	33.852	125.852	0.634	22.896%	1.342
8	10.242	802.114	9.813	4.287	42.071	154.355	0.525	27.256%	2.050
9	10.895	865.456	9.921	4.602	45.657	157.124	0.624	29.058%	2.113

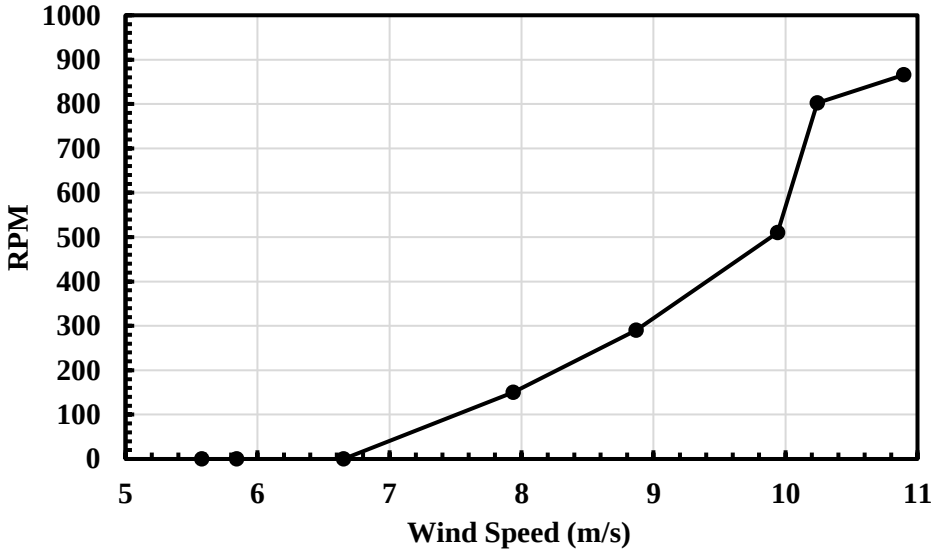

Figure 4.21 Variation of turbine speed with wind speed for Darrieus rotor

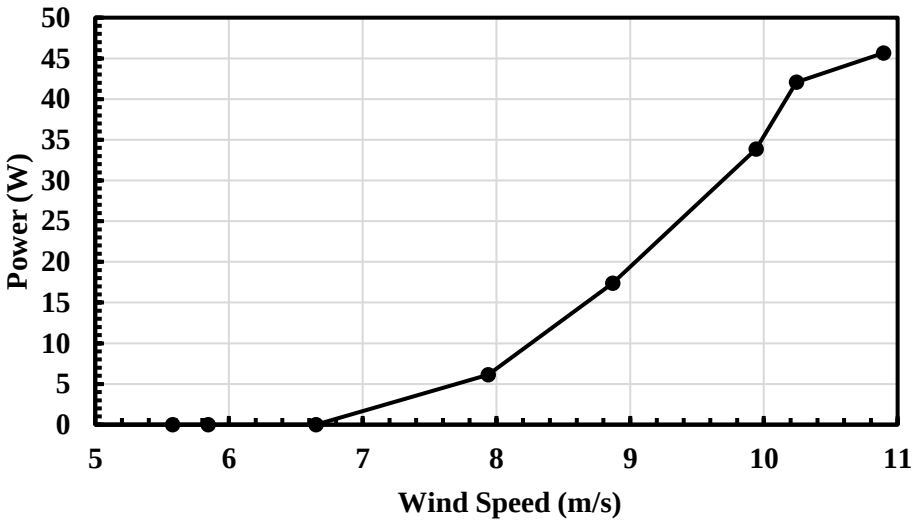

Figure 4.22 Variation of turbine power with wind speed for Darrieus rotor

In Figures 4.21 and 4.22, the variation of turbine speed and power with wind speed for the Darrieus rotor is presented. Wind speeds ranged from 3.561 m/s to 10.895 m/s. The maximum turbine speed observed was 865.456 rpm at a wind speed of 10.895 m/s. Notably, Figure 4.22 illustrates the Darrieus rotor's challenge in operating at low wind speeds. Its self-starting speed was relatively high at 7.937 m/s, necessitating a specific mechanism for initiating rotation at lower wind speed. The experimental data collected above didn't involve the utilization of such mechanism. That's why the data are left blank up to wind speed of 6.651 m/s. This limitation restricts its ability to generate sufficient power in areas with low wind speeds.

Despite the self-starting issue, the Darrieus rotor exhibited promising power generation capabilities. At a wind speed of 10.895 m/s, it achieved a maximum power output of 45.657 W. Even at a wind speed of 8.868 m/s, the Darrieus rotor generated 17.362 W, nearly double the power output of the Savonius rotor at a wind speed of 9.326 m/s, which was only 9.848 W. Furthermore, at a slightly higher wind speed of 9.941 m/s, Darrieus rotor was able to generate 33.852 W which is very high compared to that of Savonius rotor.

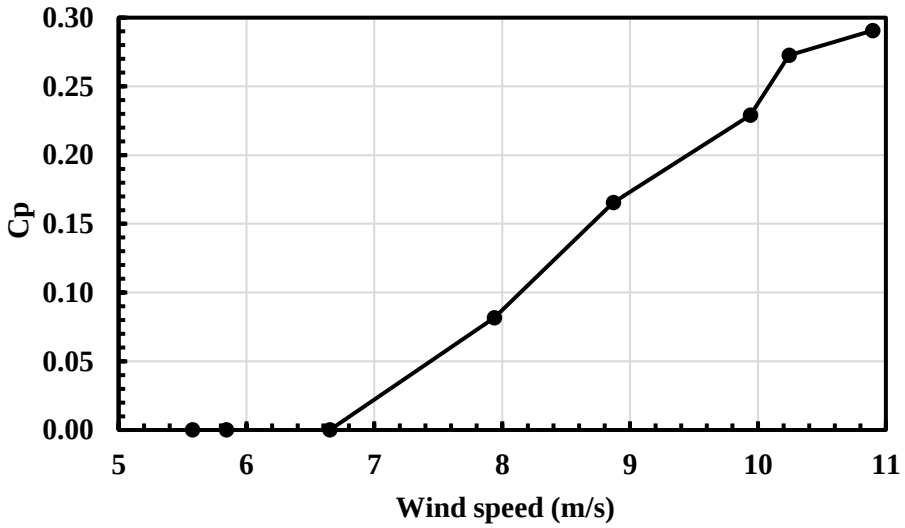

Figure 4.23 Variation of coefficient of power with wind speed for Darrieus rotor

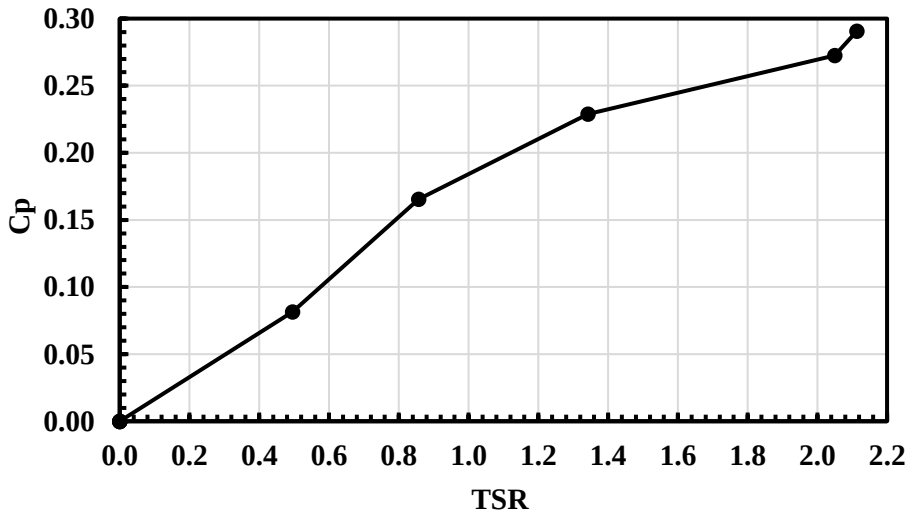

Figure 4.24 Variation of coefficient of power with TSR for Darrieus rotor

Figure 4.23 illustrates the variation of the coefficient of power (Cp) with wind speed for the Darrieus rotor. A notable maximum Cp of 29.058% was achieved at a wind speed of 10.895 m/s. Additionally, Figure 4.24 depicts the variation of Cp with Tip Speed Ratio (TSR) for the Darrieus rotor. It is observed that the TSR range for the Darrieus rotor is relatively high compared to the Savonius rotor, suggesting suitability for high-speed applications.

The maximum power coefficient attained is 29.058% at a TSR of 2.113. This value is slightly lower than the 34.83% obtained from Computational Fluid Dynamics (CFD) analysis. However, such discrepancies are anticipated due to unaccounted mechanical losses inherent in experimental measurements, particularly in power measurement.

c) Results and Discussion of Hybrid Turbine

Table 4.6 Performance Coefficient of fabricated model of Hybrid-VAWT

Experiment	Wind velocity (m/s)	rpm	Voltage (V)	Current (A)	Power Exp. (W)	Power Th. (W)	Torque Exp. (Nm)	Cp (%)	TSR
1	4.425	75.632	0.785	0.906	0.711	13.040	0.090	5.452%	0.447
2	5.624	150.864	3.203	0.688	2.205	26.771	0.140	8.235%	0.702
3	6.596	195.354	3.526	1.241	4.377	43.190	0.214	10.135%	0.775
4	7.451	355.113	6.613	1.709	11.303	62.256	0.304	18.156%	1.248
5	8.632	465.752	7.823	2.666	20.852	75.250	0.428	21.542%	1.413
6	9.186	589.561	8.252	3.421	28.229	104.958	0.508	26.896%	1.680
7	9.812	698.214	8.921	3.859	34.428	125.852	0.532	27.356%	1.863
8	10.223	815.364	9.122	4.741	43.247	154.355	0.528	28.018%	2.054
9	10.863	852.166	9.958	4.515	44.965	157.124	0.619	28.618%	2.088

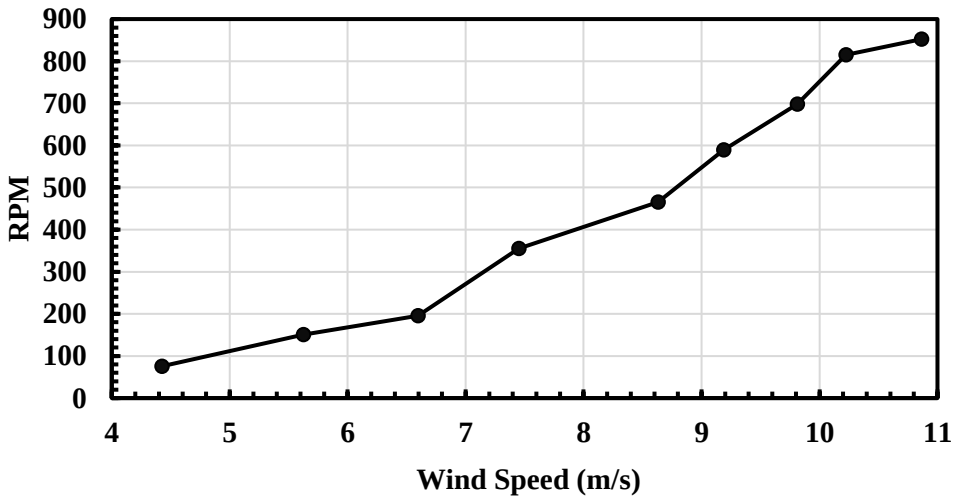

Figure 4.25 Variation of turbine speed with wind speed for Hybrid rotor

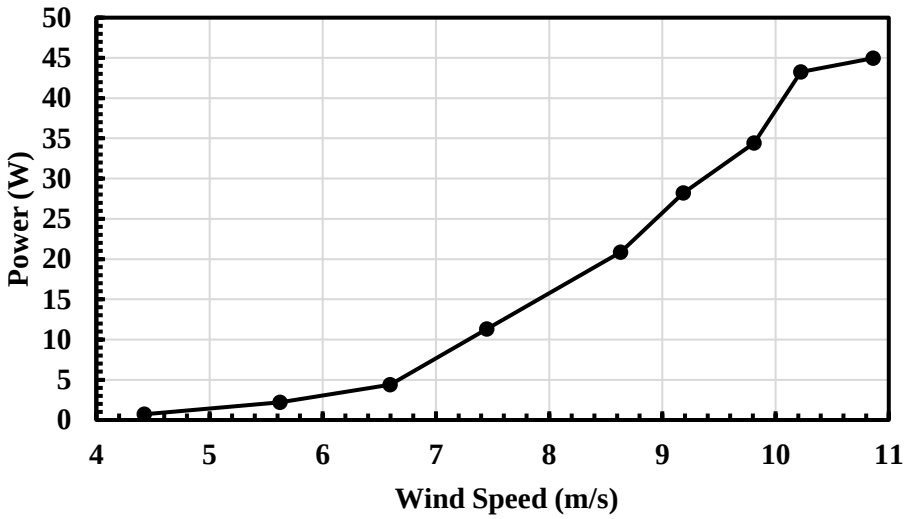

Figure 4.26 Variation of turbine power with wind speed for Hybrid turbine

Figures 4.25 and 4.26 depict the variation of turbine speed and power with wind speed for the hybrid rotor. Wind speed ranged from 4.425 m/s to 10.863 m/s. Unlike the Darrieus rotor, the hybrid rotor demonstrated the ability to operate at lower wind speeds, starting from 4.425 m/s. It was able to rotate with 75.632 rpm at wind speed of 4.425 m/s with output power of only 0.711 W. However, that's not the issue here, the main objective of this rotor was to lower the self-starting speed of Darrieus rotor to eliminate the use of external mechanism to operate it and hybrid rotor was able to meet this objective. Further, it was able to generate maximum power of about 44.965 W at wind speed of 10.863 m/s which is similar to Darrieus rotor which means hybrid rotor was able to achieve higher power output while integrating Savonius rotor. Consequently, the hybrid rotor effectively addressed the limitations of both the Savonius and Darrieus rotors. Its capability to operate at low wind speeds, comparable to the Savonius rotor, and generate higher power output, comparable to the Darrieus rotor, highlights its potential for improved wind energy conversion.

Figure 4.27 illustrates the variation of the coefficient of power (Cp) with wind speed for the Hybrid rotor. A maximum Cp of 28.618% was achieved at a wind speed of 10.863 m/s, while a minimum Cp of 5.452% was attained at the lower wind speed of

4.425 m/s. This demonstrates the Hybrid rotor's capability to operate effectively across a wide range of wind speeds, from low to high.

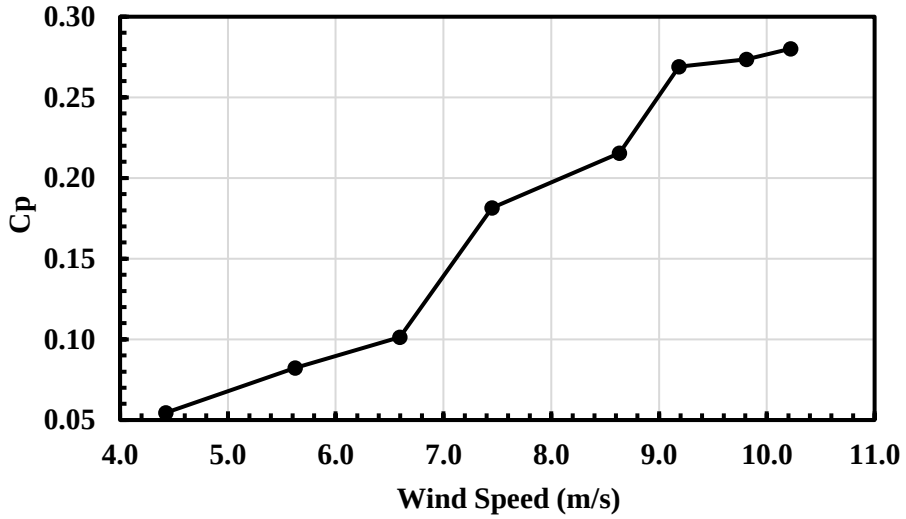

Figure 4.27 Variation of coefficient of power with wind speed for Hybrid turbine

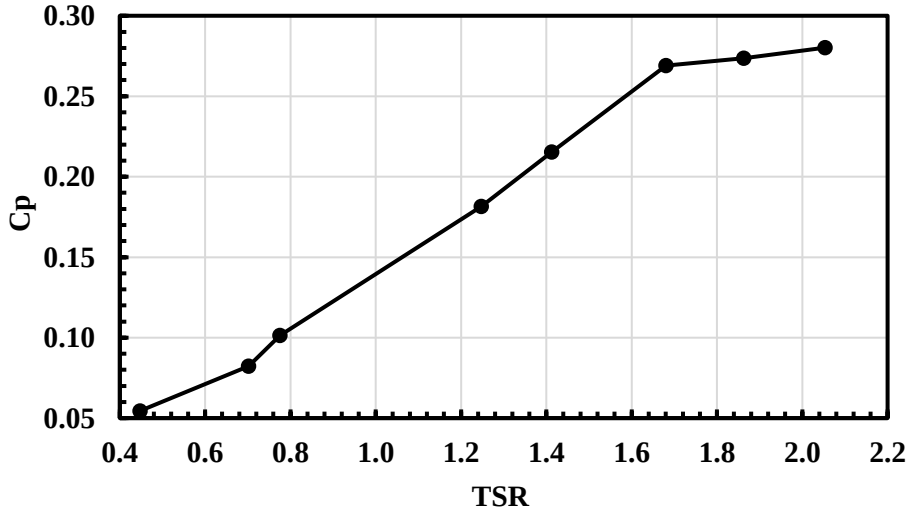

Figure 4.28 Variation of coefficient of power with Tip speed ratio for Hybrid turbine

Furthermore, Figure 4.28 displays the variation of Cp with Tip Speed Ratio (TSR) for the Hybrid rotor. It is noteworthy that the TSR range for the Hybrid rotor is comparatively high compared to the Savonius rotor, indicating its suitability for high-speed applications.

The maximum power coefficient obtained is 28.618% at a TSR of 2.088. Although this value is slightly lower than the 35.68% obtained from Computational Fluid Dynamics (CFD) analysis, such deviations are expected due to unaccounted mechanical losses inherent in experimental measurements, particularly in power assessment.

CHAPTER 5: CONCLUSION

The CFD analysis and experimental testing of Savonius, Darrieus, and hybrid rotor was successfully accomplished. Firstly, during computational fluid dynamics (CFD) investigation, number of simulations were conducted to examine the impact of the combined Darrieus-Savonius turbine's rotor radius on its performance. The outcomes indicate that altering the radius of the Savonius rotor in a combined turbine significantly influences its overall performance. The study showed that there is an optimum β at which maximum power coefficient can be achieved and further increase in β beyond that optimum value will result in decreased power coefficient. It is because the higher radius ratio increases the interaction between the Savonius and Darrieus blades and hence, the operating range of tip speed ratio is reduced. Thus, higher the dimension of Savonius bucket is, the higher the losses become; thereby the performance decreases. Based on our study the optimum β at which highest power coefficient Cp= 0.35678 achieved was β =0.43.

Similarly, after getting optimum β, simulations were performed for solo Darrieus and solo Savonius rotor and the results showed that the hybrid rotor has the ability to achieve an almost similar peak power coefficient to that of Darrieus rotors. Furthermore, Simulations were carried out at different wind speed for Darrieus and Hybrid rotors to check their self-starting ability and the results showed that hybrid rotor has the ability to start at low wind speed.

Based on the CFD analysis results, a final CAD model was designed, fabricated, and experimentally tested in a wind tunnel. The following conclusions were drawn from the experimental study:

- Coefficient of power of the Savonius turbine is 0.2193 at wind speed 8.372 m/s and it starts to decrease as wind speed increases. It is notable that the coefficient of power for Savonius rotor is quite low compared to Darrieus rotor at its highest operating wind speed. It is noteworthy that the rotor could have started at wind speeds lower than 3.438 m/s, but due to limitations of the wind tunnel, the lowest starting speed achievable was around 3.5 m/s.
- Darrieus turbine is not self-started at low wind speed as it required wind speed of 7.937 m/s to initiate the rotation but it is more efficient than the Savonius

turbine in the range of wind speed 8-11 m/s. Coefficient of power of Darrieus turbine with three aero foil blades is 0.29058 at 10.895 m/s wind speed.

- The hybrid turbine demonstrated a power coefficient of 0.10135 at a wind speed of 6.596 m/s and was capable of self-starting at 4.425 m/s, overcoming the self-starting drawback of the Darrieus turbine. Thus, the inner Savonius rotor enhanced the self-starting capability of the Darrieus rotor.
- The hybrid rotor achieved a power coefficient of 0.2862 at a wind speed of 10.863 m/s, significantly higher than that of the Savonius rotor. Introducing outer Darrieus rotors enhanced the power coefficient of the Savonius rotor.
- Discrepancies between the power obtained from CFD analysis and experimental observations were attributed to mechanical losses in the model, including fabrication errors, shaft misalignment, bearing losses, motor losses, and circuit power losses.

REFERENCES

[1] L. B. Kothe, S. V. Möller, and A. P. Petry, "Numerical and experimental study of a helical Savonius wind turbine and a comparison with a two-stage Savonius turbine," *Renew Energy*, vol. 148, pp. 627–638, Apr. 2020, doi: 10.1016/j.renene.2019.10.151.

[2] A. Zakaria and M. S. N. Ibrahim, "Turbulence modelling of a helical savonius wind turbine operating at low reynolds number," *CFD Letters*, vol. 12, no. 5, pp. 91–100, 2020, doi: 10.37934/cfdl.12.5.91100.

[3] B. Karki, A. Subedi, H. Sigdel, and P. Bartaula, "DESIGN, SIMULATION AND PERFORMANCE EVALUATION OF VERTICAL AXIS HELICAL WIND TURBINE," 2019.

[4] J. H. Lee, Y. T. Lee, and H. C. Lim, "Effect of twist angle on the performance of Savonius wind turbine," *Renew Energy*, vol. 89, pp. 231–244, Apr. 2016, doi: 10.1016/j.renene.2015.12.012.

[5] M. N. Zadeh, M. Pourfallah, S. S. Sabet, M. Gholinia, S. Mouloodi, and A. T. Ahangar, "Performance assessment and optimization of a helical Savonius wind turbine by modifying the Bach's section," *SN Appl Sci*, vol. 3, no. 8, Aug. 2021, doi: 10.1007/s42452-021-04731-0.

[6] S. Mertens, G. Van Kuik, and G. Van Bussel, "Performance of an H-Darrieus in the skewed flow on a roof," *Journal of Solar Energy Engineering, Transactions of the ASME*, vol. 125, no. 4, pp. 433–440, Nov. 2003, doi: 10.1115/1.1629309.

[7] C. S. Ferreira, G. Van Bussel, C. J. S. Ferreira, G. Van Bussel, and G. Van Kuik, "An analytical method to predict the variation in performance of a H-Darrieus in skewed flow and its experimental validation." [Online]. Available: https://www.researchgate.net/publication/259089792

[8] A. Bianchini, G. Ferrara, L. Ferrari, and S. Magnani, "An Improved Model for the Performance Estimation of an H-Darrieus Wind Turbine in Skewed Flow NOMENCLATURE ACRONYMS BEM Blade Element Momentum DMSV Double Multiple StreamTubes with Variable interference factor HAWT Horizontal Axis Wind Turbine MS Multiple StreamTubes," 2012.

[9] J. Edwards, N. Durrani, R. Howell, and N. Qin, "Wind Tunnel and Numerical Study of a Small Vertical Axis Wind Turbine," 2008.

[10] M. H. Mohamed, "Performance investigation of H-rotor Darrieus turbine with new airfoil shapes," *Energy*, vol. 47, no. 1, pp. 522–530, 2012, doi: 10.1016/j.energy.2012.08.044.

[11] R. Gupta, A. Biswas, and K. K. Sharma, "Comparative study of a three-bucket Savonius rotor with a combined three-bucket Savonius-three-bladed Darrieus rotor," *Renew Energy*, vol. 33, no. 9, pp. 1974–1981, Sep. 2008, doi: 10.1016/j.renene.2007.12.008.

[12] F. Feng, S. Li, Y. Li, and D. Xu, "Torque Characteristics Simulation on Small Scale Combined Type Vertical Axis Wind Turbine," *Phys Procedia*, vol. 24, pp. 781–786, 2012, doi: 10.1016/j.phpro.2012.02.116.

[13] S. M. Rassoulinejad-Mousavi, M. Jamil, and M. Layeghi, “Experimental study of a combined three bucket H-rotor with savonius wind turbine,” *World Appl Sci J*, vol. 28, no. 2, pp. 205–211, 2013, doi: 10.5829/idosi.wasj.2013.28.02.1429.

[14] R. K. Kavade and P. M. Ghanegaonkar, “Design and Analysis of Vertical Axis Wind Turbine for Household Application,” *Journal of Clean Energy Technologies*, vol. 5, no. 5, pp. 353–358, Sep. 2017, doi: 10.18178/JOCET.2017.5.5.397.

[15] A. Zakaria and M. S. N. Ibrahi., “Experimental Evaluation of Multiple Savonius Turbines in Oblique and Cluster Configuration,” Volume 7, No. 12 December 201//doi.org/10.30534/ijeter/2019/10712201

[16] G. Saini and R. P. Saini, “A numerical analysis to study the effect of radius ratio and attachment angle on hybrid hydrokinetic turbine performance,” *Energy for Sustainable Development*, vol. 47, pp. 94–106, Dec. 2018, doi: 10.1016/j.esd.2018.09.005.

[17] K. Sahim, D. Santoso, and D. Puspitasari, “Investigations on the Effect of Radius Rotor in Combined Darrieus-Savonius Wind Turbine,” *International Journal of Rotating Machinery*, vol. 2018, 2018, doi: 10.1155/2018/3568542.

[18] N. M. Ali, H. A. K. Abdul, and S. Aljabair, “The Effect of Darrieus and Savonius Wind Turbines Position on the Performance of the Hybrid Wind Turbine at Low Wind Speed,” *International Journal of Mechanical Engineering and Technology (IJMET)*, vol. 11, no. 2, pp. 56–72, 2020, [Online]. Available: http://www.iaeme.com/ijmet/issues.asp?JType=IJMET&VType=11&IType=2http://www.iaeme.com/IJMET/issues.asp?JType=IJMET&VType=11&IType=2Electroniccopyavailableat:https://ssrn.com/abstract=3540134http://www.iaeme.com/

[19] Siddiqui AS, Alam M, Hameed A, Nadeem S, Saleem M, and Shahzad M., “Experimental study to assess the performance of combined Savonius Darrieus vertical axis wind turbine at different arrangement,” *IEEE 21st International Multi-Topic Conference (INMIC)*, 2018, doi: 10.1109/INMIC.2018.8595538.

[20] A. P. Valerga, M. Batista, J. Salguero and F. Girot, "Influence of the PLA filament conditions on characteristics of FDM Parts," *MDPI Open access Journals,* pp. 1-3, 2018.

[21] V. Andronov, L. Beránek, V. Krůta, L. Hlavůňková and Z. Jeníková, "Overview and Comparison of PLA Filaments Commercially Available in Europe for FFF Technology," *MDPI Open Access Journal,* pp. 1-2, 2023.

[22] S.-S. Yao, F.-L. Jin, K. Y. Rhee, D. Hui and S.-j. Park, "Recent advances in carbon-fiber-reinforced thermoplastic composites: A review," *Elsevier,* vol. 142, pp. 2-3, 2018.

[23] M. N. Shojaee and M. Abbaspour, 2009, “Innovative approach to design a new national low speed wind tunnel”, Journal of Environmental Science and Engineering, ISSN:1735-1472

APPENDIX: DRAWING SHEET OF CAD MODEL

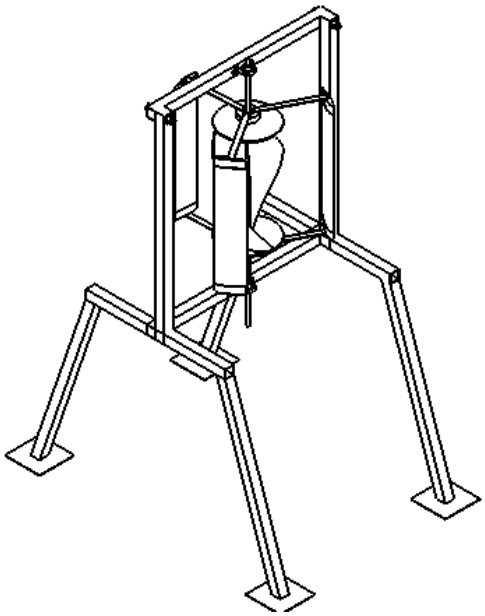

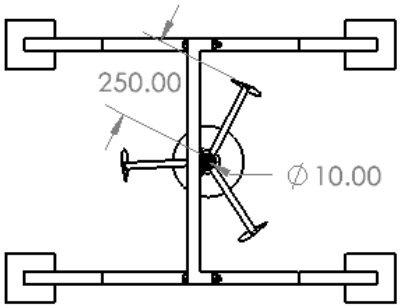

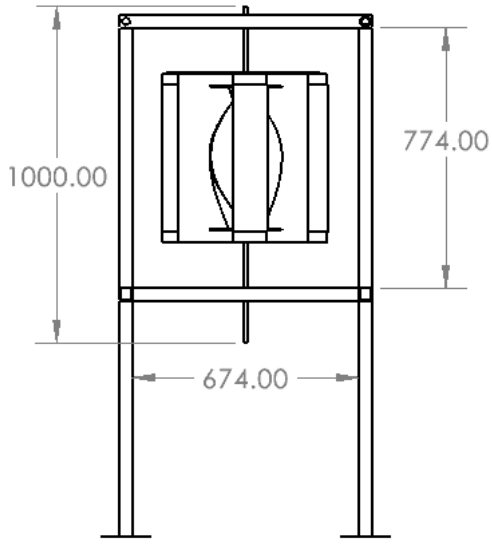

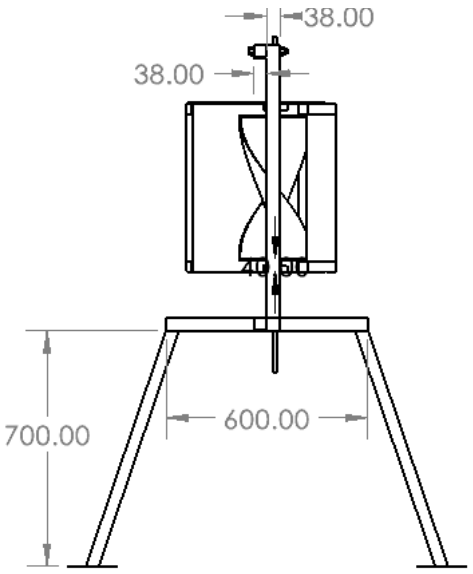

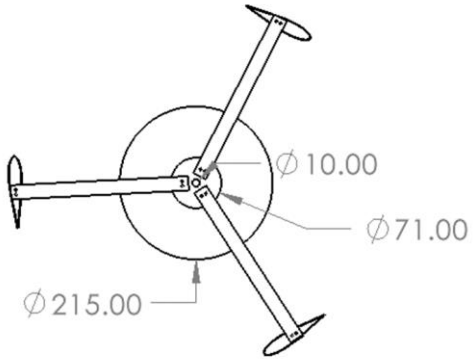

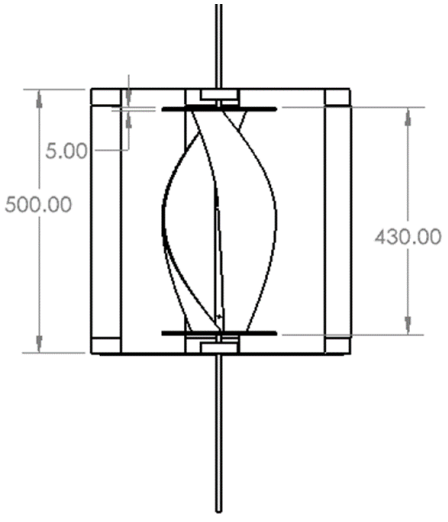

PLAGIARISM CHECK REPORT

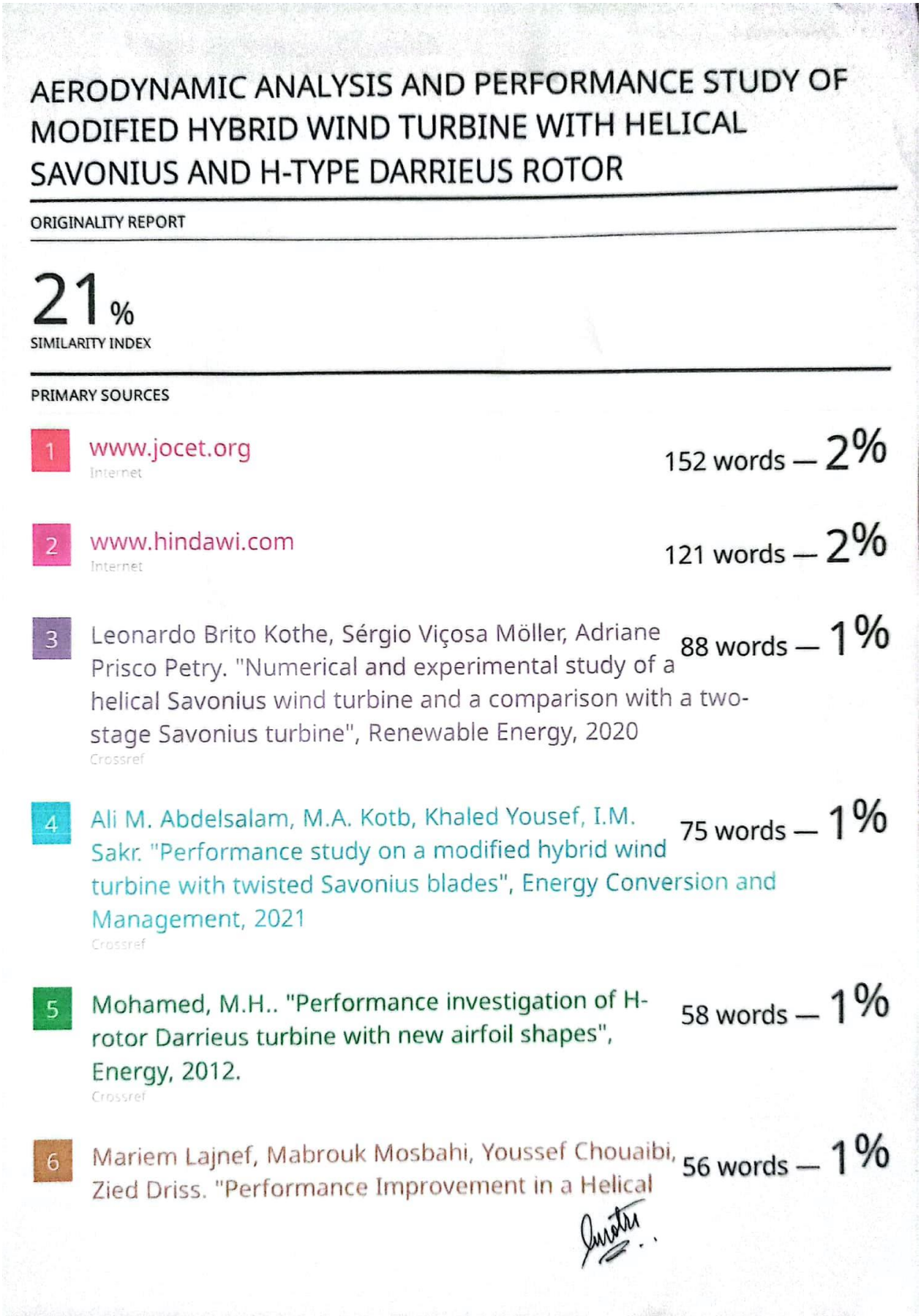

AERODYNAMIC ANALYSIS AND PERFORMANCE STUDY OF MODIFIED HYBRID WIND TURBINE WITH HELICAL SAVONIUS AND H-TYPE DARRIEUS ROTOR

ORIGINALITY REPORT

21%
SIMILARITY INDEX

PRIMARY SOURCES

1	www.jocet.org Internet	152 words — 2%
2	www.hindawi.com Internet	121 words — 2%
3	Leonardo Brito Kothe, Sérgio Viçosa Möller, Adriane Prisco Petry. "Numerical and experimental study of a helical Savonius wind turbine and a comparison with a two-stage Savonius turbine", Renewable Energy, 2020 Crossref	88 words — 1%
4	Ali M. Abdelsalam, M.A. Kotb, Khaled Yousef, I.M. Sakr. "Performance study on a modified hybrid wind turbine with twisted Savonius blades", Energy Conversion and Management, 2021 Crossref	75 words — 1%
5	Mohamed, M.H.. "Performance investigation of H-rotor Darrieus turbine with new airfoil shapes", Energy, 2012. Crossref	58 words — 1%
6	Mariem Lajnef, Mabrouk Mosbahi, Youssef Chouaibi, Zied Driss. "Performance Improvement in a Helical	56 words — 1%

Savonius Wind Rotor", Arabian Journal for Science and Engineering, 2020
Crossref

7 Bikash Karki, Ashok Subedi, Himal Sigdel, Pradeep Bartaula. "Design, simulation and performance evaluation of vertical axis helical wind turbine", Journal of Innovations in Engineering Education, 2019 — 55 words — 1%
Crossref

8 www.ijraset.com — 50 words — 1%
Internet

9 Liu, Kan. "High-Fidelity Fluid-Structure Interaction Study of the Turbine-Based Renewable Energy Harvesting Mechanism", University of Maryland, Baltimore County, 2021 — 44 words — 1%
ProQuest

10 www.coursehero.com — 39 words — < 1%
Internet

11 Sun, Xuejing. "Performance Prediction and Enhancement of the New Floating Vertical Axis Wind Turbine (VAWT)", University of Macau, 2022 — 37 words — < 1%
ProQuest

12 www.ijee.net — 36 words — < 1%
Internet

13 daneshyari.com — 32 words — < 1%
Internet

14 humaningredient.com.au — 30 words — < 1%
Internet

15 Baytekin, Erinç. "Investigation of Wake Characteristics of a Darrieus Type wind Turbine", — 29 words — < 1%